This **Supplemental Material** accompanies Curry, B.B., Kehew, A.E., Antinao, J.L., Esch, J., Huot, S., Caron, O.J., and Thomason, J.F., 2020, Deglacial Kankakee Torrent, source to sink, in Waitt, R.B., Thackray, G.D., and Gillespie, A.R., eds., Untangling the Quaternary Period—A Legacy of Stephen C. Porter: Geological Society of America Special Paper 548, https://doi.org/10.1130/2020.2548(16).

UNIVERSITY OF ILLINOIS
AT URBANA-CHAMPAIGN

Prairie Research Institute
Illinois State Geological Survey

615 East Peabody Drive
Champaign, Illinois 61820

October 19, 2015
Rev. 1.1

Luminescence dating report for Dr. Alan Kehew, from the Western Michigan University.

Extended report

ISGS code	Sample	Equivalent dose (Gy)	Dose rate (Gy/ka)	Age (ka)[a]	p (%)	n (accepted/total)
362	OSL-CA-15-01	17.1 ± 2.2	1.02 ± 0.07	17.1 ± 2.4	0	82/240
363	OSL-CA-15-02	22.1 ± 0.7	1.18 ± 0.07	18.9 ± 1.3	23	80/240
364	OSL-CA-15-03	21.1 ± 1.4	1.04 ± 0.07	19.9 ± 1.9	6	87/240
365	OSL-CA-15-04	27.1 ± 3.2	1.46 ± 0.08	18.6 ± 2.5	0	93/264

a) minimum age model

Optically stimulated luminescence (OSL) dating measured on quartz grains, in the 150 – 250 µm grains size range. Uncertainties are reported at the 1σ significance, providing a level of confidence of approximately 67 %. The uncertainties combine random and systematic errors, added in quadrature.

If all four samples represent the same geological event, then the combined age should be taken as 18.9 ± 1.3 ka (1σ).

Please note that all samples were found to be poorly-bleached at deposition. The best estimate age presented above relied on the 'minimum age model'. Full details are presented in the attached report.

Sebastien Huot, Ph.D.
Geochronology Laboratories
Illinois State Geological Survey
Champaign, IL

shuot@illinois.edu
+1-217-300-2579 (office)

This is a report for the optically stimulated luminescence dating (OSL) of four samples, delivered to us by Alan Kehew, from the Western Michigan University, on July 1, 2015. They were retrieved in opaque steel tubes. These samples came from active sand and gravel quarry, related to the formation of the Kalamazoo Moraine, tied to the Saginaw Lobe. They would have been deposited approximately 17 ka years ago, or possibility within a 14 to 20 ka age range. The depositional environment are interpreted as a supraglacial lake (OSL-CA-15-01), a glaciofluvial (OSL-CA-15-02 and OSL-CA-15-03) and a lacustrine origin (OSL-CA-15-04). All four samples are expected to be partially bleached, prior to burial, which would lead to an age overestimation is not properly taken into account. For purpose of internal identification, we labeled these as ISGS 362 to 365.

1. Sample preparation and equipment

The tubes were opened and the mineral extraction processed in a subbed orange light environment. One inch of sediment was removed from both ends of the tube, as these might be partial exposed to light during sampling. Sediment from these external portions were used to measure the *in situ* water content and its radioactive content (uranium, thorium and potassium), both for dose rate calculation. Quartz minerals for OSL dating were extracted from the remainder (inner portion) of each tube.

These were wet sieved, to retrieve the 150 – 250 µm grain size. A hydrochloric acid attack (HCl, 10 %) was applied to dissolve any carbonate minerals that might be present. Using a heavy liquid solution of lithium heteropolytungstate (LST), at 2.61 g/ml, we separated K-feldspar and albite (> 2.61) from quartz minerals (< 2.61). For quartz, further purification was made with a hydrofluoric acid attack (HF, 48 % for 1 hour), to dissolve any remaining impurities. A second HCl attack was perform, to dissolve calcium fluorite minerals, a potential by-product of HF dissolution of Ca-rich silicates. Finally, the purified quartz extracts were again sieved, at 150 µm, to remove partially dissolved impurities. A purity check was performed by doing an infrared over blue OSL stimulation. These samples showed no significant contamination from feldspar.

For dose rate, sediments from the external portion of each sampling tubes were dried and a representative portion was encapsulated in petri dishes (~ 20 – 23 g) and sealed with paraffin wax. A minimum waiting time of 21 days after sealing is recommended to restore the radioactive equilibrium of radon 222 daughter products (Gilmore, 2008). The specific activity (Bq/kg) were measured with a broad energy high purity germanium detector (BEGe), in a planar configuration, shielded by 15 cm thick lead. Efficiency calibration for the detector was obtained with a set of 4 certified standards (IAEA-RGU-1, IAEA-RGTh-1, IAEA-RGK-1 and IAEA-385).

2. Dose rate

Waiting times from 31 to 38 days were observed before measuring the radioactive activities of uranium, thorium and potassium, from which we can derive contributions from alpha, beta and gamma energy decay (Table 1, 2). We assumed an internal content of 0.08 ± 0.02 ppm and 0.18 ± 0.03 ppm, for uranium and thorium respectively (Vandenberghe et al., 2008). A conservative 0.04 ± 0.02 "a value" (efficiency of alpha particles compared to beta particle at inducing a trapped charge in quartz and feldspar; i.e. alpha as a 4 % efficiency) was retained. The external alpha dose rate contribution is assumed negligible here, since we etched the quartz grains. The beta dose rate absorption efficiencies were adjusted according to the grain size, 150 – 250 µm (Nathan, 2011). The beta dose rate contribution were further adjusted for one hour of HF etch (i.e. 10 µm etch dissolution depth). External beta and gamma contributions were attenuated for water content (Zimmerman, 1971). Energy to dose rate conversion coefficient relied on the Guérin et al. (2011) update.

Table 1. Specific activity (Bq/kg).

	sample (ISGS code)			
	362	363	364	365
238U	3.8 ± 0.8	8.1 ± 1.2	6.7 ± 1.3	9.7 ± 1.4
226Ra	7.4 ± 0.3	11.3 ± 0.4	10.9 ± 0.4	9.4 ± 0.4
210Pb	10.8 ± 1.5	9.1 ± 1.5	8.2 ± 1.4	14 ± 2
232Th	4.7 ± 0.3	9.8 ± 0.2	7.3 ± 0.3	7.0 ± 0.2
40K	228 ± 6	254 ± 7	238 ± 7	373 ± 9

Table 2. Contribution to the dose rate, expressed in Gy/ka. We relied on a 12 ± 5 % water content.

sample	Alpha Internal	Beta External	Gamma	Cosmic ray	depth (m)	Total
362	0.01 ± 0.01	0.56 ± 0.04	0.273 ± 0.018	0.18 ± 0.05	2	1.02 ± 0.07
363	0.01 ± 0.01	0.66 ± 0.05	0.37 ± 0.02	0.14 ± 0.05	4	1.18 ± 0.07
364	0.01 ± 0.01	0.61 ± 0.05	0.33 ± 0.02	0.08 ± 0.05	10	1.04 ± 0.07
365	0.01 ± 0.01	0.87 ± 0.07	0.41 ± 0.02	0.17 ± 0.05	2.4	1.46 ± 0.08

The water content were measured for each sample. The 'as received' water content were quite low, at 5 – 6 % (over dry sediment), for samples ISGS 362, 363 and 365. Sample ISGS 364 was more humid, at 10 %. We hypotheses that these samples would have been relatively humid, but never fully saturated. For calculation, we attributed conservative values of water content, of 12 ± 5 %. '12' is halfway between completely dry and fully saturated. We are uncertain, though.

3. Equivalent dose (De)

For the equivalent doses (De) measurements, we relied on an automated Risø TL-DA-20 system, equipped with a set of blue (470 nm) and infrared (870 nm) LEDs, for light stimulation. Detection was made in the UV (Hoya U340 filter) for quartz. For each samples, we dispensed quartz grains over a very small area (1 mm), onto a silicon oil covered stainless disk (10 mm diameter). Around 10 - 20 grains were dispensed on each disk. A total of 240 or 264 aliquots were measured, for each samples.

OSL measurements were carried out with a S.A.R. protocol (Table 3). Its optimal measurement parameters were selected by a dose recovery test (latent dose bleached twice with blue LEDs, at 125°C). An initial dose was given at first (being a close match to the measured equivalent dose for each sample; 48 Gy, ISGS 362; 34 Gy, ISGS 363; 20 Gy, ISGS 364; 27 Gy, ISGS 365) and subsequently recovered by measuring its equivalent dose with a S.A.R. protocol (Figure 1). The samples responded well to the treatment, giving a measured to given dose ratio of 1.09 ± 0.12, 0.99 ± 0.03, 1.04 ± 0.03 and 1.02 ± 0.03, for sample 362 to 365, all with an overdispersion of 0 %, for the selected preheat temperatures (200 or 220°C). This is very good. Considering this, we opted to select the parameters in table 3. The overdispersion is a parameter that quantifies the amount of scatter, beyond what can be predicted from the observations. A 20 % overdispersion is considered 'normal'. It does, however, indicates that our measurement uncertainties are too small. This is a subject of on-going research in luminescence dating.

Table 3. Measurement steps for the single aliquot regenerative protocol (Murray and Wintle, 2000). [a]) For equivalent dose measurements, we gave a range of laboratory-induced dose that would properly encompass the variability of the observed natural luminescence. A preheat of 220°C was used (except for sample 364, where we took 200°C), along with a cut heat of 180°C (except for sample 364, where it was 160°C).

1. Regeneration [a]/Natural dose
2. Preheat (200 or 220°C), held for 10 seconds
3. OSL stimulation with blue light at 100°C for 40 seconds (L_x)
4. Test dose beta irradiation (7 Gy)
5. Cut heat (160 or 180°C) for 0 sec
6. OSL stimulation with blue light at 100°C for 40 seconds (T_x)
7. Repeat Steps 1-6 with further regeneration doses

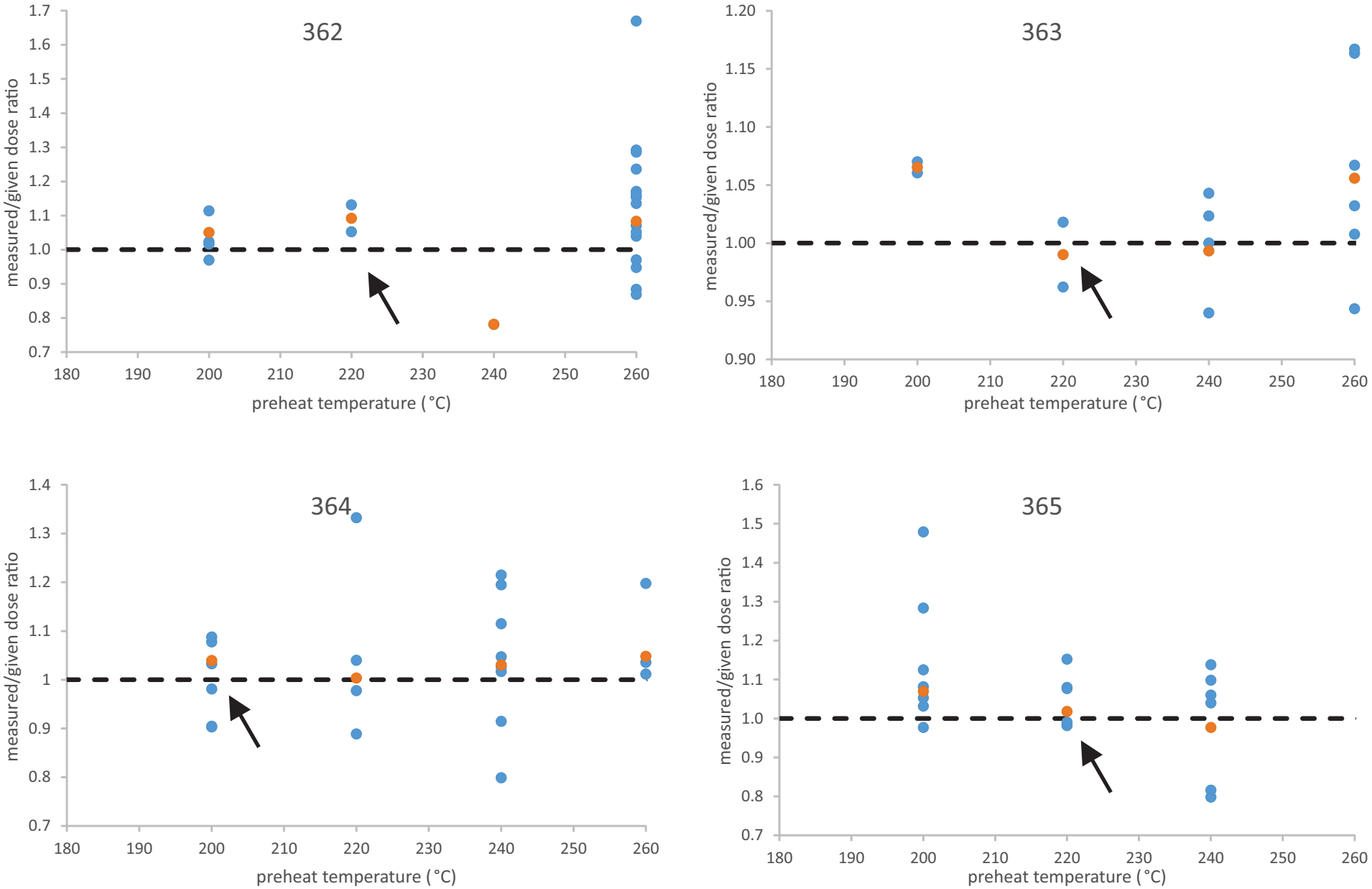

Figure 1. Result for the dose recovery test. Individual aliquots (blue circles) and their weighted mean (orange circles) are shown, for different preheat temperature (i.e. step 2 of Table 3). The arrow points to the preheat temperature that was retained for measuring the equivalent dose (burial age) for the sediments. Luminescence dating tolerance tends to be conservative. For the dose recovery, we allow up to 10 % variation from unity (i.e. 0.9 – 1.1).

For the equivalent dose, all calculations were made using the "late light" approach for background subtractions, by taking the initial 5 data channels (0.8 second) from the OSL decay curve and removing a background from the end of the stimulation curve (50 data channels; 8 seconds; figure 2). Aliquots were rejected (table 4), due to feldspar contamination (10 % threshold limit) or high recuperation (5 % limit of the natural luminescence). Most were rejected, however, because they showed very low luminescence intensities, barely discernable from the instrumental background.

Table 4. Tally of rejected aliquots.

ISGS code	n (accepted/total)	feldspar contaminated	high recuperation	dim
362	82/240	18	1	139
363	80/240	19	5	136
364	87/240	6	5	142
365	93/264	32	2	137

Uncertainties relied on Poisson statistics. For curve fitting, we also propagated the uncertainties from the optimized parameters. Also, when the observed scatter about the best fit regression line was too high the uncertainties were increased (Figure 3). For this, we relied on the one-tail probability χ^2 distribution, with a N-3 degree of freedom (where N is the number of measured data point). When the probability was lower than 15 % (i.e., the data point scatter above and beyond the best fit line), the uncertainties for the optimized parameters were expanded by the Student's-t value for N-3 degrees of freedom (Brooks et al., 1972; Ludwig, 2003).

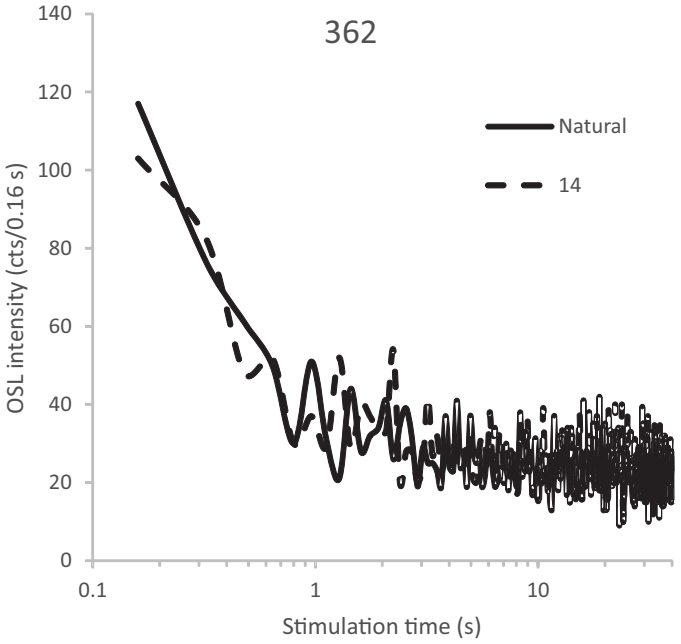

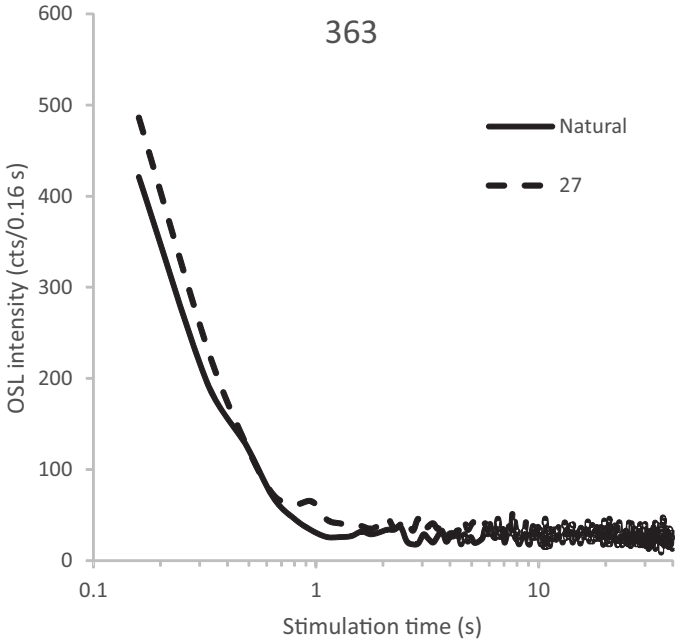

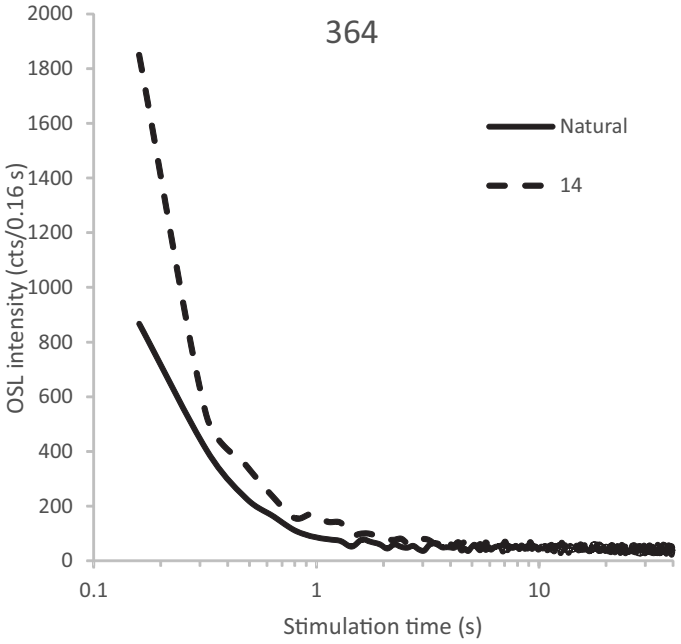

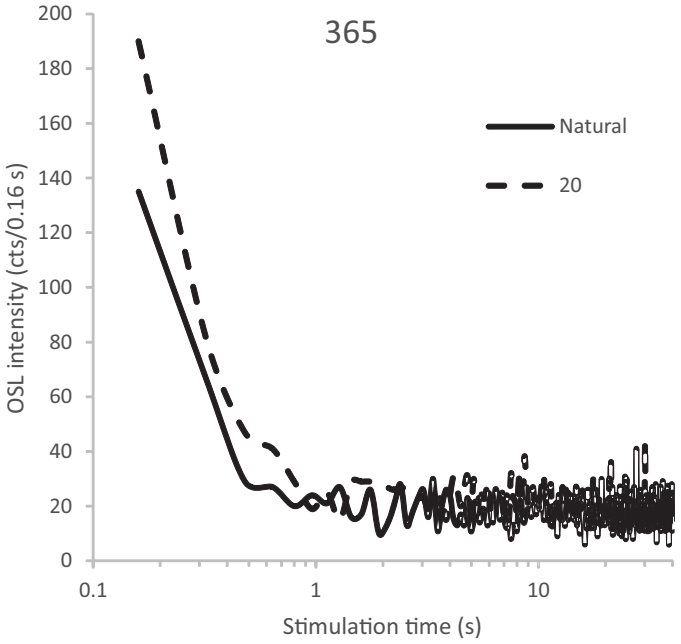

Figure 2. Typically OSL decay curve, for a naturally dose aliquot (solid curve) or laboratory-induced dose (dashed curve, in Gy). The area under the curve is proportional to the dose of radiation stored within the mineral. Despite being of a low light intensity, these aliquots gave age estimates falling within the minimum age. Their luminescence growth curve are shown in Figure 3.

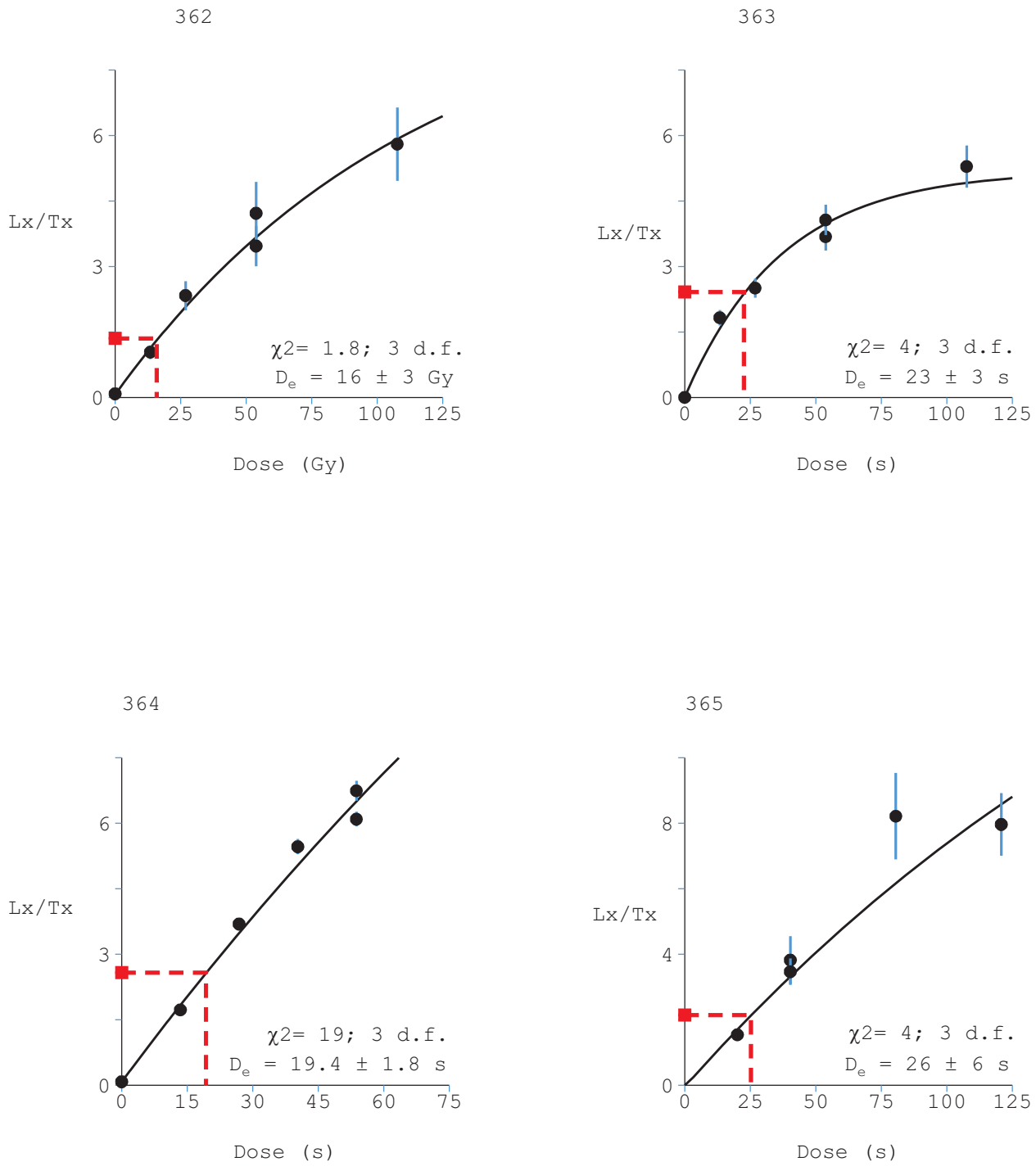

Figure 3. Luminescence dose response curve, for the same aliquots shown in Figure 2. Each point correspond to OSL (Lx; measurement step 3) of a natural (red square) or laboratory-induced dose (black circle), normalized by the luminescence response to a fixed test dose (Ti; measurement step 6). The equivalent dose is obtained by interpolation. For the aliquot shown for sample 364, the data scatters beyond the statistical predictability, with a reduced Chi2 of 6.3 (18.87/3), giving a 0.03 % probability of fit. For the others shown here, the observed measurements scatters well around the predicted model. Granted, these are not the finest of quartz OSL, but this is what the data looks like, for these samples. These aliquots were picked at random, from the population that was 'well-bleached', at deposition.

A weighted average (using the central age model; Galbraith et al., 1999) was used in all calculations, except when noted otherwise. The central age model provides an overdispersion parameter. The overdispersion characterize the degree by which the observed weighted distribution is consistent with the expected weighted distribution. At 0 %, the observed distribution is equal to the statistical prediction. In luminescence dating, it is common for the observed distribution to be slightly larger than the expected, by a value of approximately 20 %. This means that our calculated uncertainties tends to underestimate the 'real' uncertainties, due to intrinsic (such as instrumental uncertainties) or extrinsic factors (such as partial bleaching, external micro-dosimetry). The central age model expands the age uncertainty, in an attempt to take into account this discrepancy. Here, the overdispersion are modest to high, ranging from 32 ± 5 up to 86 ± 10 % (at 1σ; table 5), which means this is a large scatter in the calculated age distribution, aside, perhaps, for OSL-CA-15-02!

Table 5. Age overdispersion parameters. A value of 20 % is typical in luminescence.

ISGS code	Sample	Overdispersion (%)
362	OSL-CA-15-01	86 ± 10
363	OSL-CA-15-02	32 ± 5
364	OSL-CA-15-03	61 ± 8
365	OSL-CA-15-04	70 ± 8

Most samples display a significant positive skewness (Figure 4), except, perhaps, for OSL-CA-15-03. This sample is relatively well distributed. Given that these sediments came from a relatively proximal distance from a glacial moraine, it is not surprising that a portion of the quartz grains were insufficiently exposed to sunlight (a few seconds up to a few minutes, of direct sunlight, is required), during their last sediment cycle (erosion, transport, sedimentation). In order to more clearly document the shape of the age distribution we must reduce the amount of quartz grains dispensed on each aliquot. Otherwise, in the presence of a multitude of quartz grains on one aliquot (some being well-bleached, others, not so), each emitting a luminescence light signal, all these will sum up and will give an age over-estimation (Arnold and Roberts, 2009). The only recourse here is to severely reduce the amount of grains dispensed on the aliquot (Olley et al., 1999). At the extreme limit, we would measure the luminescence from a single grain.

The best tool for this is the Risø single grain laser attachment. Unfortunately, the ISGS lab does not possess that attachment (in fact, very few OSL lab have such a device). As an alternative, we rely on the 'poor's man approach', which consist of dispensing a very small amount of grain on each aliquot, and hope for the best! How it can work is quite simple: most quartz grains are insensitive to radiation and/or yield extremely low luminescence light intensities (Preusser et al., 2009). In a typical sediment, we can expect that, on average, only 5 % of any quartz grain to yield decent luminescence characteristics (sufficient luminescence light intensity, successful recycling and recuperation tests; Duller, 2008). With this in mind, if we dispense 20 quartz grains on an aliquot, we would detect a luminescence signal from only 1 grain.

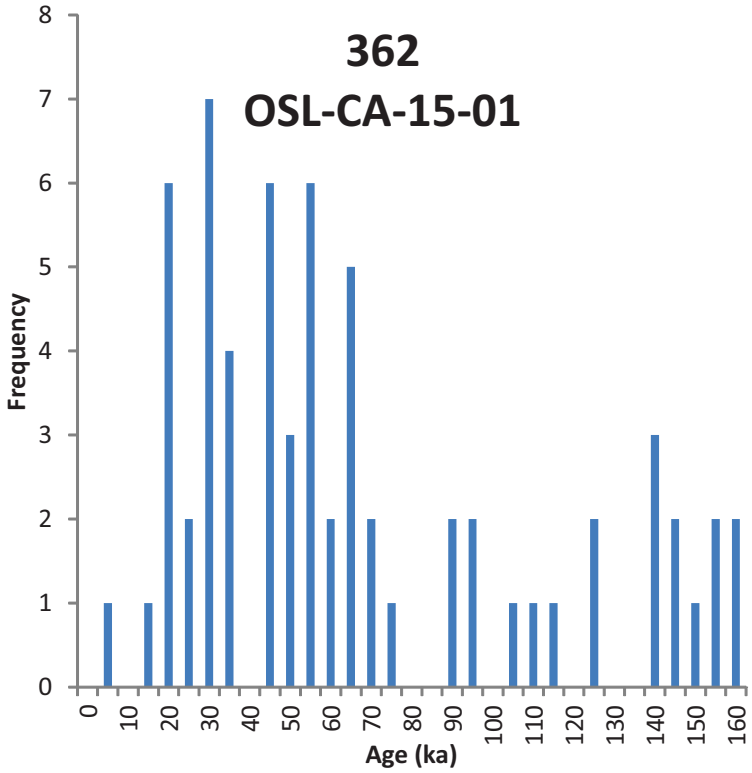

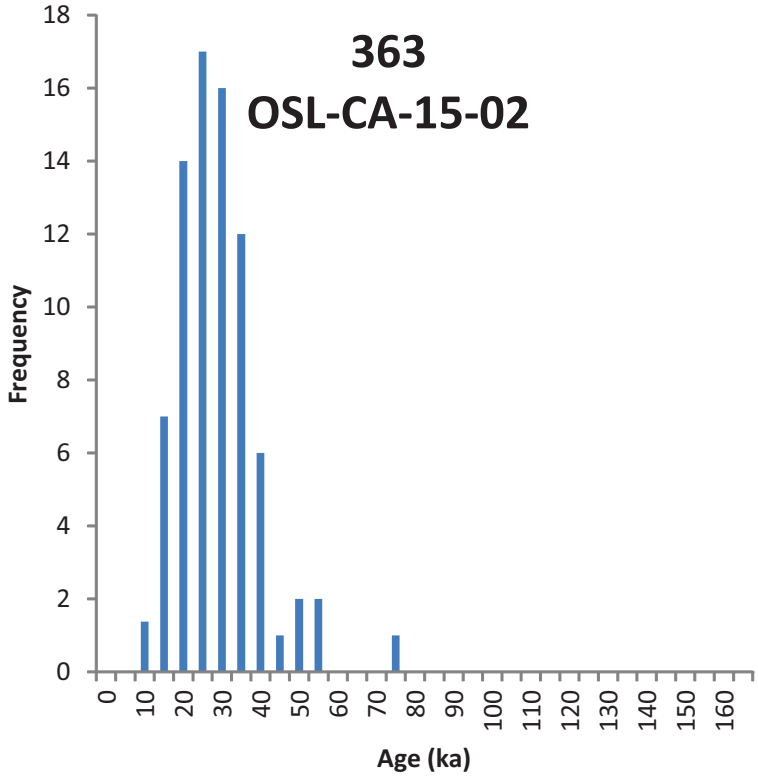

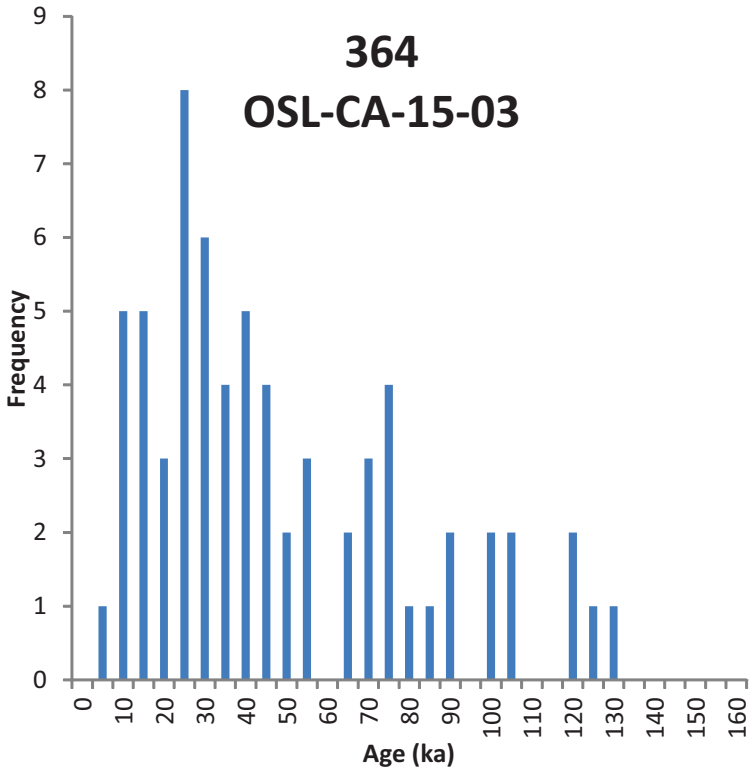

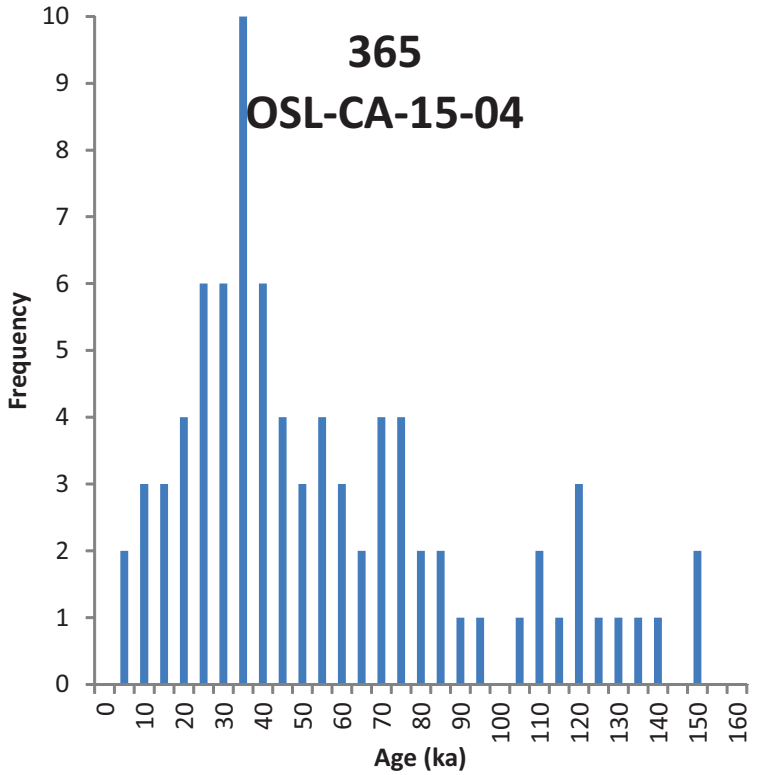

Figure 4. Age distributions.

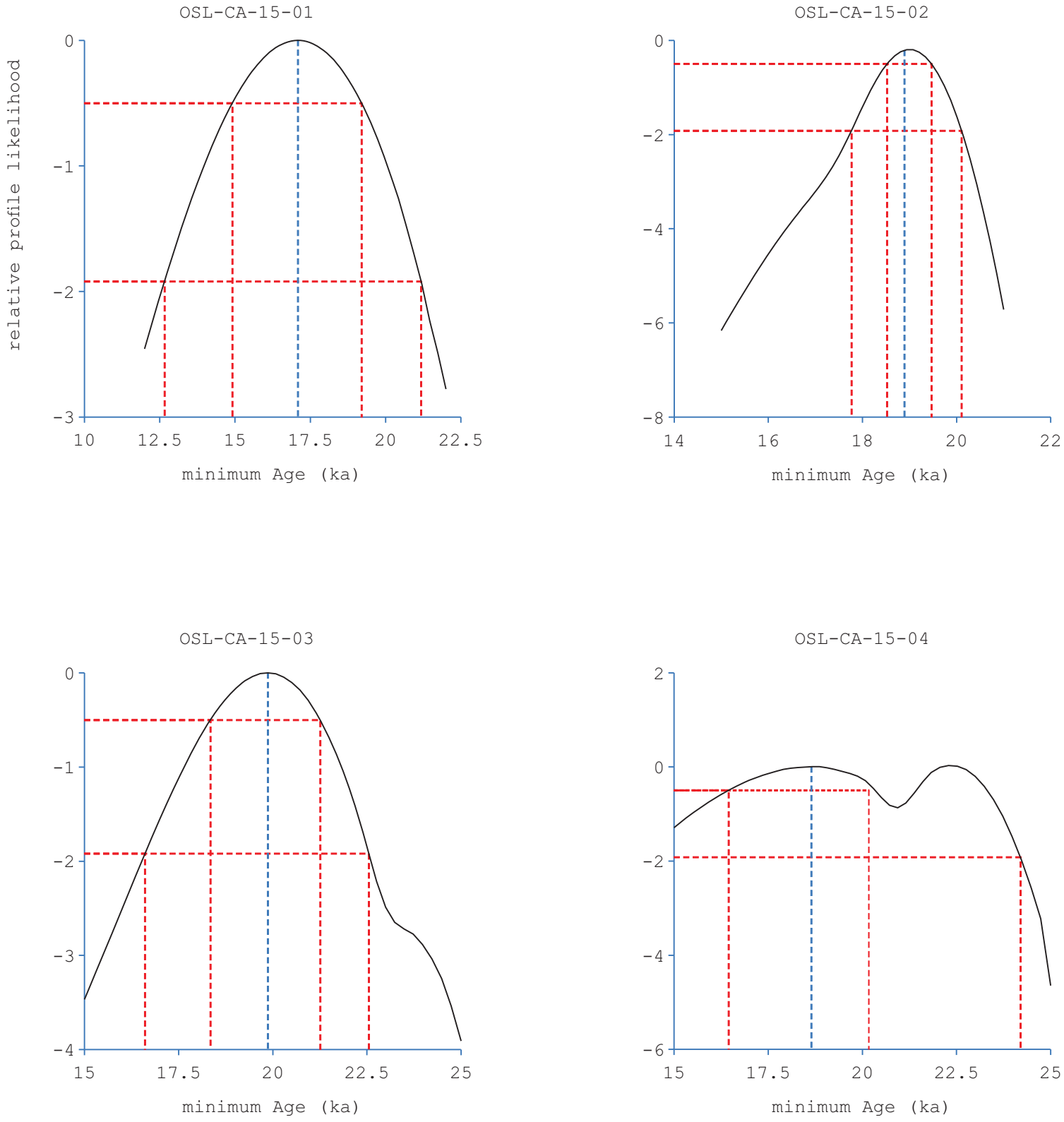

Figure 5. Relative profile likelihood. The minimum age is found at the maximum value of the profile (dotted blue line). The 1 and 2σ uncertainties are shown by the red dotted lines..

To increase our confidence that, whenever we see a measurable luminescence signal, it only comes from 1 grain, we made sure that a significant number of aliquot provided no measurable (or very low) luminescence light signal. For all samples, between 41 and 48 % of the measured aliquots yielded no (or very low) luminescence light signal (Table 4). Hence, that condition is fulfilled.

Usually, the best age estimate should rely on the average value. We can think of instances where this might be inappropriate. A positive skewness, such as is noted here for most samples, is a clear sign of partial bleaching. In other words, during the last sedimentary cycle (erosion, transport, deposition and burial), not all sedimentary grains were sufficiently exposed to sunlight, to completely reset the 'dosimetric clock', that they had accumulated in their previous burial setting. Whereas the mean is the scientist's best friend, it might prove to be an inappropriate estimator in some situations. Here, we opted to rely on the minimum age model (Galbraith et al., 1999). We choose not to add an additional uncertainty (σb), in quadrature to each individual aliquots before inserting them into the minimum age model, since the data already have a low precision. The minimum burial age falls between 17 and 20 ka (Figure 5; Table 3). For sample OSL-CA-15-02, despite being poorly bleached, it has a decent amount of grains in agreement with the minimum age (p = 23 %). On the other hand, samples OSL-CA-15-01 and OSL-CA-15-04 are poorly defined.

Table 3. Burial age comparison between the weighted mean (central age model) and minimum age model.

ISGS	Sample	Weighted mean (ka)	Minimum age model (ka)	p (%)
362	OSL-CA-15-01	61 ± 8	17.1 ± 2.4	0
363	OSL-CA-15-02	28 ± 2	18.9 ± 1.3	23
364	OSL-CA-15-03	42 ± 4	19.9 ± 1.9	6
365	OSL-CA-15-04	68 ± 8	18.6 ± 2.5	0

3.1 Uncertainty budget

The breakdown of the uncertainties, between the total random and systematic sources, are presented in table 4. If all four samples represent the same geological event, then the combined age should be taken as 18.9 ± 1.3 ka (1σ), by treating separately the random and systematic uncertainty contribution.

Table 4. Random and systematic uncertainties, at 1 sigma.

ISGS code	sample	Age	uncertainty random	uncertainty systematic	uncertainty total
362	OSL-CA-15-01	17.1	2.2	1.1	2.4
363	OSL-CA-15-02	18.9	0.6	1.1	1.3
364	OSL-CA-15-03	19.9	1.4	1.3	1.9
365	OSL-CA-15-04	18.6	2.2	1.0	2.5

4. Conclusion

In summary, all four samples shows pronounced signs of having being poorly-bleached, during their last sedimentary cycle. There were not especially bright in their luminescence light-response. Our best age estimated is provided by the minimum age model, with 17.1 ± 2.4, 18.9 ± 1.3, 19.9 ± 1.9 and 18.6 ± 2.5 ka, for sample OSL-CA-15-01 through OSL-CA-15-04. The large uncertainties stems from the low luminescence intensities measured here and also because only a portion of the measured aliquots were identified as being well-bleached at deposition, before their last burial. The only way to further reduce the uncertainty is to significantly increase the number of measured aliquots. It is, however, beyond the scope of current mandate.

Sebastien Huot
Visiting Research Scholar - Geochemistry
Geochronology Laboratories
Illinois State Geological Survey

References

Arnold, L.J., Roberts, R.G., 2009. Stochastic modelling of multi-grain equivalent dose (De) distributions: Implications for OSL dating of sediment mixtures. Quaternary Geochronology 4, 204-230.
Brooks, C., Hart, S.R., Wendt, I., 1972. Realistic use of two-error regression treatments as applied to rubidium-strontium data. Reviews of Geophysics 10, 551-577.
Duller, G.A.T., 2008. Single-grain optical dating of Quaternary sediments: why aliquot size matters in luminescence dating. Boreas 37, 589-612.
Galbraith, R.F., Roberts, R.G., Laslett, G.M., Yoshida, H., Olley, J.M., 1999. Optical dating of single and multiple grains of quartz from Jinmium rock shelter, northern Australia: part I, experimental design and statistical models. Archaeometry 41, 339-364.
Gilmore, G.R., 2008. Practical gamma-ray spectrometry, 2nd ed. John Wiley & Sons, Ltd.
Guérin, G., Mercier, N., Adamiec, G., 2011. Dose-rate conversion factors: update. Ancient TL 29, 5-8.
Ludwig, K.R., 2003. Mathematical-statistical treatment of data nd errors for Th-230/U geochronology, in: Bourdon, B., Henderson, G.M., Lundstrom, C.C., Turner, S.P. (Eds.), Uranium-Series Geochemistry. Mineralogical Society of America, pp. 631-656.
Murray, A.S., Wintle, A.G., 2000. Luminescence dating of quartz using an improved single-aliquot regenerative-dose protocol. Radiation Measurements 32, 57-73.
Nathan, R.P., 2011. Numerical modelling of environmental dose rate and its application to trapped-charge dating, Social Sciences Division; University of Oxford. School of Archaeology; St. Hugh's College. University of Oxford, p. 207.
Olley, J.M., Caitcheon, G.G., Roberts, R.G., 1999. The origin of dose distributions in fluvial sediments, and the prospect of dating single grains from fluvial deposits using optically stimulated luminescence. Radiation Measurements 30, 207-217.
Preusser, F., Chithambo, M.L., Götte, T., Martini, M., Ramseyer, K., Sendezera, E.J., Susino, G.J., Wintle, A.G., 2009. Quartz as a natural luminescence dosimeter. Earth-Science Reviews 97, 184-214.
Vandenberghe, D., De Corte, F., Buylaert, J.P., Kučera, J., Van den haute, P., 2008. On the internal radioactivity in quartz. Radiation Measurements 43, 771-775.
Zimmerman, J., 1971. The radiation-induced increase of the 100°C thermoluminescence sensitivity of fired quartz. Journal of Physics C: Solid State Physics 4, 3265-3276.

UNIVERSITY OF ILLINOIS
AT URBANA-CHAMPAIGN

Prairie Research Institute
Illinois State Geological Survey

615 East Peabody Drive
Champaign, Illinois 61820

December 5, 2016

Luminescence dating report for Alan Kehew, from the Western Michigan University.

ISGS code	Sample	Grain Size (µm)	Equivalent dose (Gy)	Dose rate (Gy/ka)	Age (ka)
493	CASS-OSL-16-01	150 - 250	26.6 ± 1.1	1.34 ± 0.07	19.8 ± 1.3
494	CASS-OSL-16-02	150 - 250	24.4 ± 1.7	1.38 ± 0.06	17.7 ± 1.5

Optically stimulated luminescence (OSL) dating was measured on quartz grains, on small aliquots. Uncertainties are reported at a 1σ significance, providing a level of confidence of approximately 67%. The uncertainties combine random and systematic errors, added in quadrature.

Further details can be found in the report.

Sebastien Huot, Ph.D.
Illinois State Geological Survey
Champaign, Illinois
shuot@illinois.edu
+1-217-300-2579 (office)

This is a report on the optically stimulated luminescence (OSL) dating of two samples delivered to us by Alan Kehew, on November 9th, 2016. The samples were retrieved in opaque tubes from excavated trenches or natural exposure. The depositional environment is interpreted as an ice-walled lake plain sediment. These are presumed to have been partially bleached prior to burial, which would lead to an age overestimation if not properly taken into account. For the purposes of internal identification, we labeled these samples ISGS 493 and 494.

1. Sample preparation and equipment

The tubes were opened and the mineral extraction was conducted in a subdued orange light environment. One inch of sediment was removed from both ends of the tube because these might have been partially exposed to light during sampling. Sediment from the external portions was used to measure the *in situ* water content and its radioactive content (uranium, thorium, and potassium), both for dose rate calculation. Quartz minerals for OSL dating were extracted from the remainder (inner portion) of each tube. Additional material was supplied for the external (gamma) dose rate by sampling the surrounding sedimentary unit.

These minerals were wet sieved to retrieve the 150- to 250-µm grain size. A hydrochloric acid attack (HCl, 10%) was applied to dissolve any carbonate minerals that might be present. Using a heavy liquid solution (2.62 g/mL) of lithium heteropolytungstate (LST), we separated K-feldspar and albite (>2.62) from the quartz minerals (<2.62). For quartz, further purification was done with a hydrofluoric acid (HF) attack (48% for 1 hour) to dissolve any remaining impurities. A second HCl attack was performed to dissolve calcium fluorite minerals, a potential by-product of HF dissolution of Ca-rich silicates. Finally, the purified quartz extracts were again sieved, at 150 µm, to remove partially dissolved impurities. A purity check was performed by doing an infrared over blue OSL stimulation. These quartz samples showed no significant contamination from feldspar.

To obtain the dose rate, sediments from the external portion of each sampling tube were dried, and a representative portion was encapsulated in petri dishes (~20 g) and sealed with paraffin wax. A minimum waiting time of 21 days after sealing is recommended to restore the radioactive equilibrium of radon-222 daughter products (Gilmore, 2008). The specific activities (Bq/kg) were measured with a broad-energy high-purity germanium detector (BEGe), in a planar configuration, shielded by 15 cm of thick lead. Efficiency calibration of the detector was obtained with a set of four certified standards (IAEA-RGU-1, IAEA-RGTh-1, IAEA-RGK-1, and IAEA-385).

2. Equivalent dose (De) measurements

For the equivalent doses (De) measurements, we relied on an automated Risø TL-DA-20 system, equipped with a set of blue (470 nm) and infrared (870 nm) LEDs, for light stimulation. Detection was made in the UV (Hoya U340 filter) for quartz. For each samples, we dispensed quartz grains over a very small area (1 mm), onto a silicon oil covered stainless disk (10 mm diameter). Around 10 - 20 grains were dispensed on each disk. A total of 240 aliquots were measured, for each quartz samples.

OSL measurements were carried out with a single-aliquot regenerative dose (SAR) protocol (Table 1). The optimal measurement parameters were selected by a dose recovery test (latent dose bleached twice with blue LEDs, at 125°C), for 100 for quartz. An initial dose was given at first (that was a close match to the measured equivalent dose for each sample; from 40 Gy) and it was subsequently recovered by measuring its equivalent dose with the SAR protocol (Figure 1). The samples responded reasonably well to the treatment. The optimal measurement treatment was verified for each sample. From this we selected a preheat temperature (Lx) of 240°C (held for 10 seconds). The preheat temperature for the test dose (Tx) was 200°C. The dose recovery test was performed for every sample using the most appropriate temperature (Figure 1). It yielded an average measured-to-given dose ratios of 0.95 ± 0.03, for quartz. This outcome is positive. Considering this result, we opted to select the parameters in Table 1.

Table 1. Measurement steps for the single-aliquot regenerative protocol (Murray and Wintle, 2000; 2003)[1]

Step	Procedure (quartz)
1	Regeneration[1]/natural dose
2	Preheat (240°C), hold for 10 seconds
3	OSL stimulation with blue LEDs at 100°C for 40 seconds (L_x)
4	Test dose beta irradiation (10 Gy)
5	Cut heat (200°C) for 0 seconds
6	OSL stimulation with blue LEDs at 100°C for 40 seconds (T_x)
7	Repeat Steps 1–6 with further regeneration doses

[1]For equivalent dose measurements, we gave a range of laboratory-induced doses that would properly encompass the variability of the observed natural luminescence.

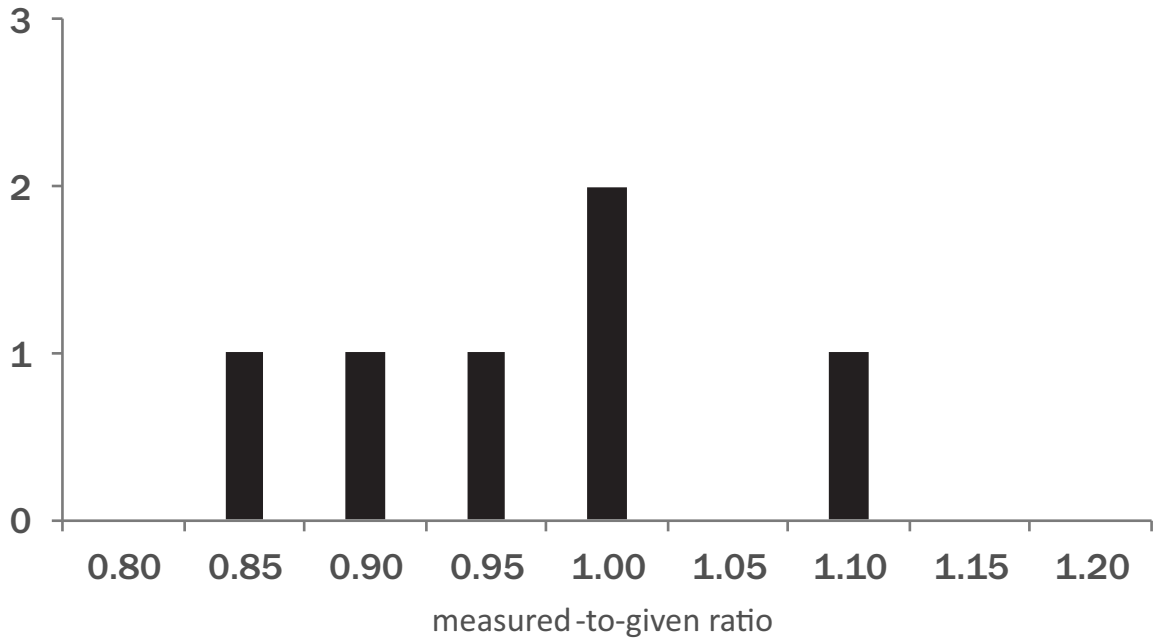

Figure 1. Summary for the dose recovery for every sample, for its selected and retained preheat temperature, for quartz. Luminescence dating tolerance tends to be conservative. For the dose recovery, we allow up to 10% variation from unity (i.e., 0.9 – 1.1).

For the equivalent dose, all calculations were made using the "late light" approach for background subtractions, by taking the initial 10 data channels (5 seconds) from the OSL decay curve and removing the background from the end of the stimulation curve for quartz (25 data channels, 12.5 seconds; Figure 2). Quartz aliquots were rejected (Table 2) because of feldspar contamination (10% threshold limit) or high recuperation (5% limit of the natural luminescence). In addition, numerous aliquots were rejected for having a low fast-ratio (Durcan and Duller, 2011).

Table 2. Tally of rejected aliquots.

ISGS code	Sample	n (accepted/total)	feldspar contaminated	recuperation	OSL decay shape	no signal
493	CASS-OSL-16-01	37/240	7	2	29	165
494	CASS-OSL-16-02	15/96	5	0	20	56

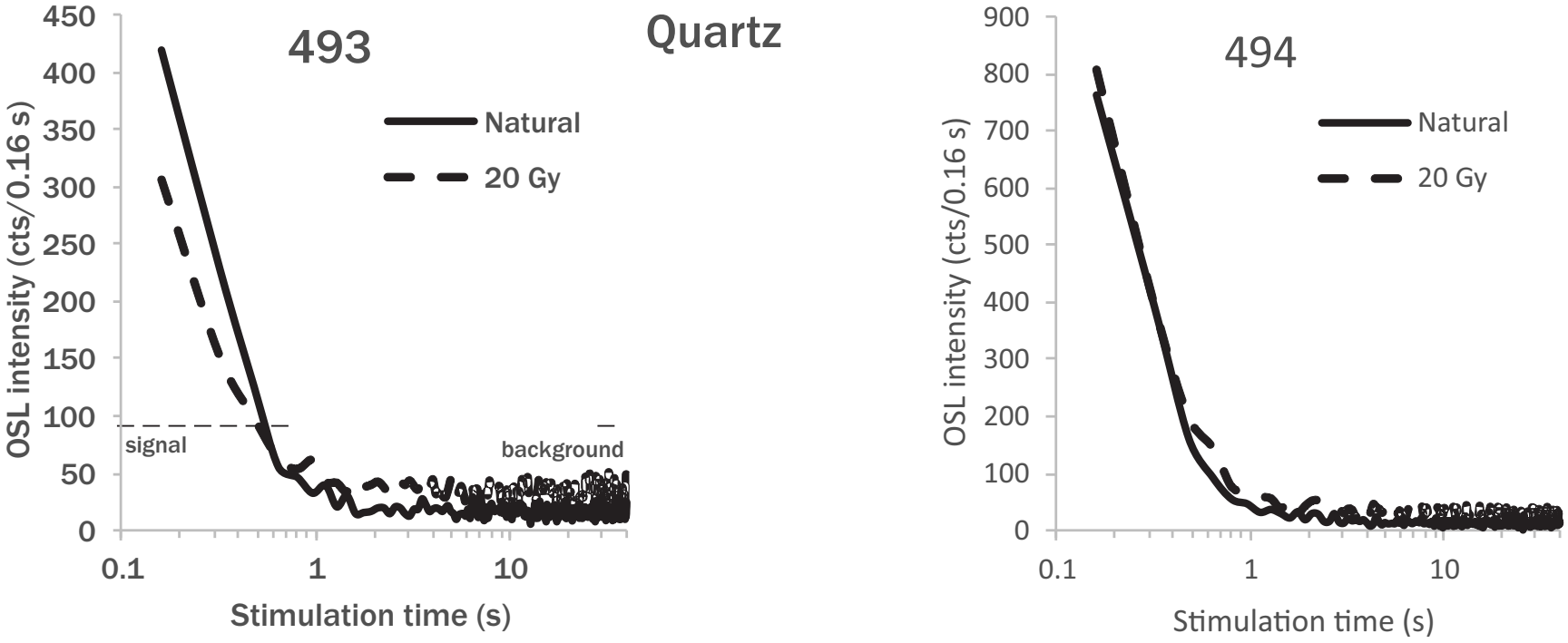

Figure 2. Typically OSL decay curve, for a naturally dose aliquot (solid curve) or laboratory-induced dose (dashed curve, in Gy). The area under the curve is proportional to the dose of radiation stored within the mineral. Their luminescence growth curve are shown in Figure 3.

2.1 Equivalent dose calculation

Uncertainties relied on Poisson statistics. For curve fitting, we also propagated the uncertainties from the optimized parameters. In addition, when the observed scatter about the best fit regression line was too high, the uncertainties were increased (Figure 3). For this, we relied on the one-tailed probability χ^2 distribution, with N – 3 degrees of freedom (where N is the number of measured data points). When the probability was lower than 15% (i.e., the data points scattered above and beyond the best fit line), the uncertainties for the optimized parameters were expanded by Student's *t* values for N – 3 degrees of freedom (Brooks et al., 1972; Ludwig, 2003).

A weighted average (using the central age model; Galbraith et al., 1999) was used in all calculations, except when noted otherwise. The central age model provides an overdispersion parameter. This parameter characterizes the degree to which the observed weighted distribution is consistent with the predicted weighted distribution from the observed data. At 0%, the observed distribution is equal to the statistical prediction. In luminescence dating, it is common for the observed distribution to be slightly larger than the expected distribution by a value of approximately 20%. This means that our calculated uncertainties tend to underestimate the "real" uncertainties because of intrinsic (e.g., instrumental uncertainties, anomalous fading) or extrinsic (e.g., partial bleaching, external microdosimetry, dose rate) factors. The central age model expands the age uncertainty in an attempt to take this discrepancy into account. Here, the overdispersions are within the average (Table 3).

Table 3. Age overdispersion parameters[1]

ISGS code	Sample	Overdispersion (%)
493	CASS-OSL-16-01	21 ± 3
494	CASS-OSL-16-02	22 ± 5

[1]A value of 20% is typical in luminescence.

Both samples displayed a normal age distribution (Figure 4). There might have a weak, older tail, put this is poorly defined. We expected these sediments to be poorly-bleached. What this means is that the age of the source sediment (before the last sedimentary cycle) must have been young and well-bleached. Alternatively, it could be that the sedimentary process that led to this body of sediment was very efficient in exposing all quartz grains to sufficient sunlight before burial.

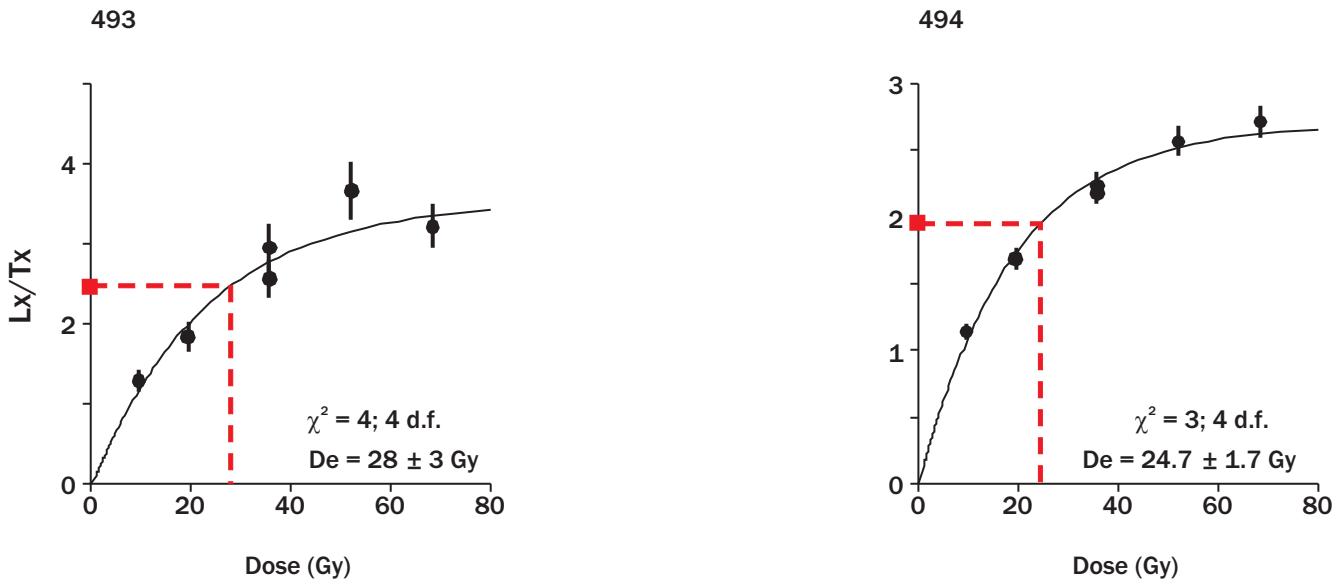

Figure 3. Luminescence dose response curve for the same aliquots shown in Figure 2. Each point corresponds to the OSL (Lx; measurement step 3 (quartz)) of a natural (red square) or laboratory-induced dose (black circles), normalized by the luminescence response to a fixed test dose (Ti; measurement step 6 (quartz)). The equivalent dose is obtained by interpolation. For the aliquots shown here, the observed measurements scatter well around the predicted best-fit curve.

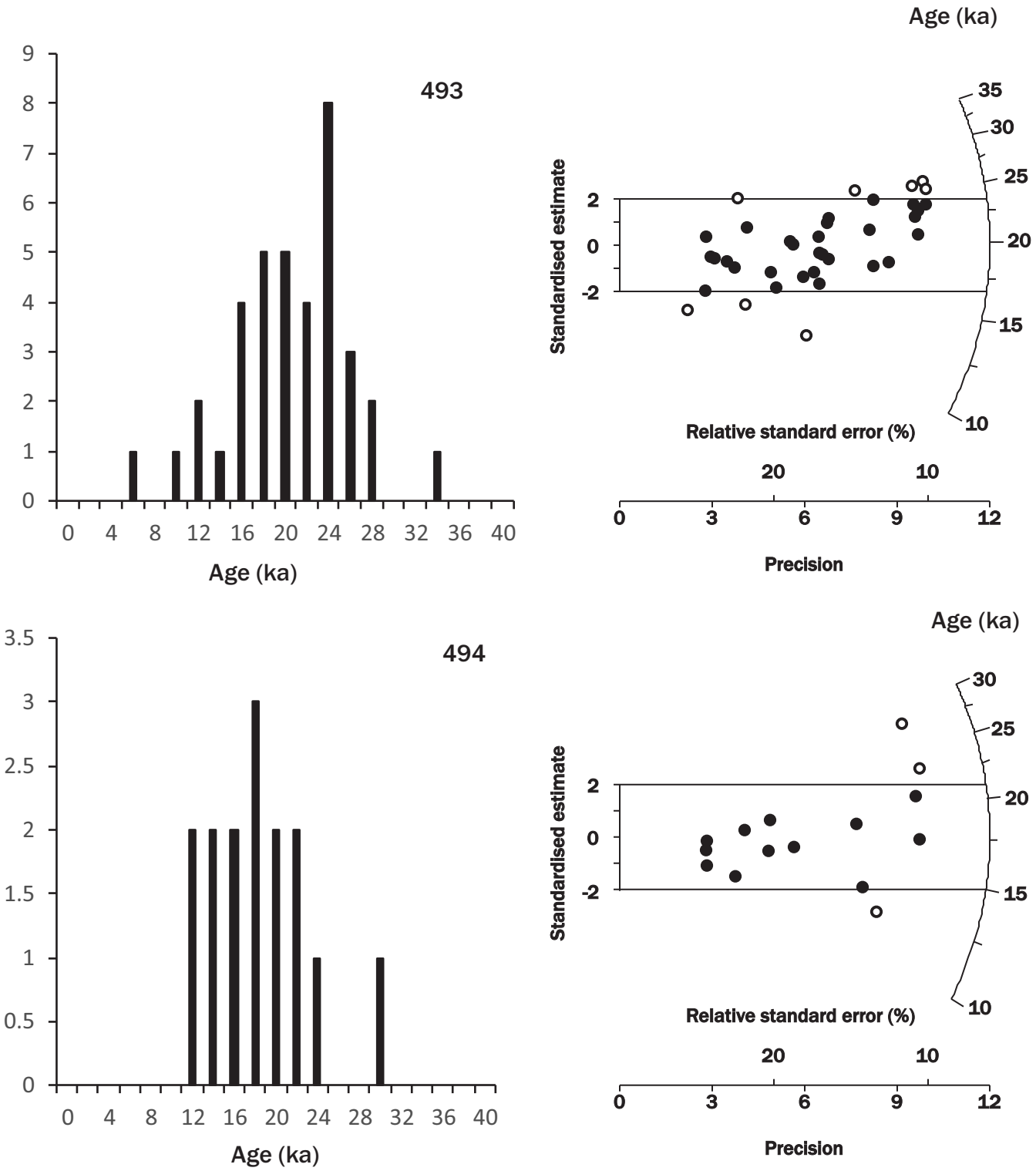

Figure 4. Age distributions, as an histogram and a radial plot, for all samples. Each circle on the radial plot represents the age and uncertainty, for a single aliquot. The age is read on the arc axis, by drawing a straight line from 0,0, passing through a circle and intersecting the arc-axis. The 0,0 coordinate corresponds to the 0 standardised estimate (y-axis) and 0 precision (x-axis). The uncertainty is read on the horizontal axis, by drawing a perpendicular line reaching the red symbol. Hence, two aliquots, having the same age, but with different uncertainty, will line on the same straight line (0,0 to the arc-axis). The aliquot with the small uncertainty will be closer to the arc. The two horizontal lines, at 2 and -2 standardised estimate, represent the 2σ standard deviations, for an horizontal age line. A cluster of aliquots within these two lines express confidence that we have a population of aliquots consistent with a single age (filled circles). For each plot, that horizontal line at 0 standardised estimate (not shown) corresponds to the weighted age.

3. Dose rate

The water content was measured for each sample. The as-received water content was relatively dry to humid (Table 4). On discussing the issue with Peixian Shu we opted for the values presented in the table. We assigned a water content uncertainty of 5 % to account for possible variation during the entire length of burial.

Table 4. Water content, measured from the sample, along with the value presumed to have prevailed during the burial

ISGS code	Sample	in situ (OSL tube) (%)	film roll capsule (%)	presumed (%)
493	CASS-OSL-16-01	4	13	13
494	CASS-OSL-16-02	5	15	15

Waiting times of 21 days were observed before measuring the radioactive activities of uranium, thorium, and potassium, from which we can derive contributions from alpha, beta, and gamma energy decay (Table 5). Some sample contained a large amount of large clasts. For dose rate calculations we had to separate the larger than 2 mm grain size fraction and measure its uranium, thorium and potassium content, distinct from the lower than 2 mm fraction. The content from smaller grains were used to evaluate the alpha, beta and gamma dose rate, whereas the larger grains were only used to evaluation their contribution to the gamma dose rate (Aitken, 1998; Urbanova et al., 2015). The relative gamma dose rate contribution, from the smaller and larger grain size, was weighted by their respective fractional mass (Figure 5).

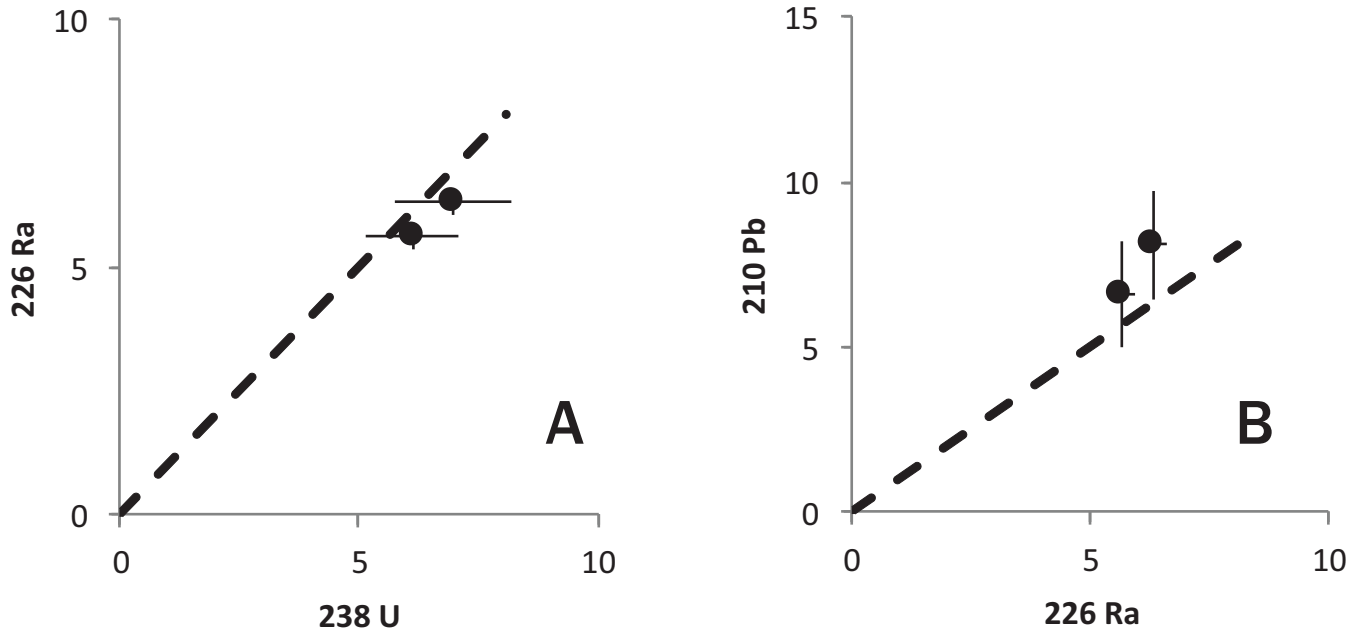

Figure 5. Specific activity (Bg/kg) for uranium 238, radium 226 and lead 210, for all samples. A), relationship of radium 226 versus uranium 238. B), relationship of lead 210 versus radium 226. The dashed line represents the 1:1 ratio. If a sample is in equilibrium, then the daughter isotope (y-axis) will match the activity of its parent (x-axis). Uncertainties are shown for 1σ.

Table 5. Specific activity (Bq/kg)

ISGS code	Sample	238U	226Ra	210Pb	232Th	40K
493	CASS-OSL-16-01	6.1 ± 1.0	5.6 ± 0.3	6.6 ± 2	5.9 ± 0.2	375 ± 8
494	CASS-OSL-16-02	7.0 ± 1.2	6.3 ± 0.3	8 ± 2	6.0 ± 0.2	374 ± 8

For quartz, we assumed an internal content of 0.08 ± 0.02 ppm and 0.18 ± 0.03 ppm, for uranium and thorium, respectively (Vandenberghe et al., 2008). A conservative 0.04 ± 0.02 "a value" (efficiency of alpha particles compared with beta particles upon inducing a trapped charge in quartz and feldspar; i.e., alpha is only 4% as effective as beta) was retained. The external alpha dose rate contribution was assumed to be negligible here because we etched the quartz grains (Table 7).

Table 6. Contribution to the dose rate, expressed in Gy/ka[1]

sample	Beta External	Gamma	Cosmic ray	depth (m)	Water Content (%)	Total
493	0.83 ± 0.06	0.36 ± 0.01	0.13 ± 0.01	4.6	13 ± 5	1.33 ± 0.06
494	0.83 ± 0.06	0.37 ± 0.01	0.18 ± 0.01	1.8	14 ± 5	1.38 ± 0.06

[1]We relied on an internal alpha dose rate of 0.01 ± 0.01 for quartz.

The beta dose rate absorption efficiencies were adjusted according to the specific grain size and mineral used for equivalent dose measurement (Nathan, 2011). For quartz, the beta dose rate contribution was further adjusted for one hour of HF etching (i.e., at a 10-μm etch dissolution depth). External beta and gamma contributions were attenuated for water content (Zimmerman, 1971). The energy-to-dose rate conversion coefficient relied on the update by Guérin et al. (2011).

4. Conclusion

In summary, both samples appeared well-bleached during their last sedimentary cycle. The quartz from these samples were in general well-behaved, but some were rejected aliquots. The ages relied only on those quartz aliquots that displayed suitable luminescence characteristics.

Our best age estimates were provided by a weighted mean (the central age model).

Sebastien Huot
Visiting Research Scholar - Geochemistry
Illinois State Geological Survey

References

Aitken, M.J., 1998. An introduction to optical dating. Oxford University Press, Oxford.

Arnold, L.J., Roberts, R.G., 2009. Stochastic modelling of multi-grain equivalent dose (De) distributions: Implications for OSL dating of sediment mixtures. Quaternary Geochronology 4, 204-230.

Auclair, M., Lamothe, M., Huot, S., 2003. Measurement of anomalous fading for feldspar IRSL using SAR. Radiation Measurements 37, 487-492.

Brooks, C., Hart, S.R., Wendt, I., 1972. Realistic use of two-error regression treatments as applied to rubidium-strontium data. Reviews of Geophysics 10, 551-577.

Cunningham, A.C., Wallinga, J., 2010. Selection of integration time intervals for quartz OSL decay curves. Quaternary Geochronology 5, 657-666.

Duller, G.A.T., 2008. Single-grain optical dating of Quaternary sediments: why aliquot size matters in luminescence dating. Boreas 37, 589-612.

Durcan, J.A., Duller, G.A.T., 2011. The fast ratio: A rapid measure for testing the dominance of the fast component in the initial OSL signal from quartz. Radiation Measurements 46, 1065-1072.

Galbraith, R.F., Roberts, R.G., Laslett, G.M., Yoshida, H., Olley, J.M., 1999. Optical dating of single and multiple grains of quartz from Jinmium rock shelter, northern Australia: part I, experimental design and statistical models. Archaeometry 41, 339-364.

Gilmore, G.R., 2008. Practical gamma-ray spectrometry, 2nd ed. John Wiley & Sons, Ltd.

Guérin, G., Mercier, N., Adamiec, G., 2011. Dose-rate conversion factors: update. Ancient TL 29, 5-8.

Huntley, D.J., Baril, M.R., 1997. The K content of the K-feldspars being measured in optical dating or in thermoluminescence dating. Ancient TL 15, 11-13.

Huntley, D.J., Hancock, R.G.V., 2001. The Rb contents of the K-feldspar grains being measured in optical dating. Ancient TL 19, 43-46.

Huntley, D.J., Lamothe, M., 2001. Ubiquity of anomalous fading in K-feldspars and the measurement and correction for it in optical dating. Canadian Journal of Earth Sciences 38, 1093-1106.

Huot, S., Lamothe, M., 2003. Variability of infrared stimulated luminescence properties from fractured feldspar grains. Radiation Measurements 37, 499-503.

Jain, M., Murray, A.S., Bøtter-Jensen, L., 2003. Characterisation of blue-light stimulated luminescence components in different quartz samples: implications for dose measurement. Radiation Measurements 37, 441-449.

Ludwig, K.R., 2003. Mathematical-statistical treatment of data nd errors for Th-230/U geochronology, In: Bourdon, B., Henderson, G.M., Lundstrom, C.C., Turner, S.P. (Eds.), Uranium-Series Geochemistry. Mineralogical Society of America, pp. 631-656.

Murray, A.S., Wintle, A.G., 2000. Luminescence dating of quartz using an improved single-aliquot regenerative-dose protocol. Radiation Measurements 32, 57-73.

Murray, A.S., Wintle, A.G., 2003. The single aliquot regenerative dose protocol: potential for improvements in reliability. Radiation Measurements 37, 377-381.

Nathan, R.P., 2011. Numerical modelling of environmental dose rate and its application to trapped-charge dating, Social Sciences Division; University of Oxford. School of Archaeology; St. Hugh's College. University of Oxford, p. 207.

Olley, J.M., Caitcheon, G.G., Roberts, R.G., 1999. The origin of dose distributions in fluvial sediments, and the prospect of dating single grains from fluvial deposits using optically stimulated luminescence. Radiation Measurements 30, 207-217.

Preusser, F., Chithambo, M.L., Götte, T., Martini, M., Ramseyer, K., Sendezera, E.J., Susino, G.J., Wintle, A.G., 2009. Quartz as a natural luminescence dosimeter. Earth-Science Reviews 97, 184-214.

Rhodes, E.J., 2000. Observations of thermal transfer OSL signals in glacigenic quartz. Radiation Measurements 32, 595-602.

Urbanova, P., Hourcade, D., Ney, C., Guibert, P., 2015. Sources of uncertainties in OSL dating of archaeological mortars: The case study of the Roman amphitheatre “Palais-Gallien” in Bordeaux. Radiation Measurements 72, 100-110.

Vandenberghe, D., De Corte, F., Buylaert, J.P., Kučera, J., Van den haute, P., 2008. On the internal radioactivity in quartz. Radiation Measurements 43, 771-775.
Wintle, A.G., 1973. Anomalous fading of thermoluminescence in mineral samples. Nature 245, 143-144.
Wintle, A.G., Murray, A.S., 2006. A review of quartz optically stimulated luminescence characteristics and their relevance in single-aliquot regeneration dating protocols. Radiation Measurements 41, 369-391.
Zimmerman, J., 1971. The radiation-induced increase of the 100°C thermoluminescence sensitivity of fired quartz. Journal of Physics C: Solid State Physics 4, 3265-3276.

UNIVERSITY OF ILLINOIS
AT URBANA-CHAMPAIGN

Prairie Research Institute
Illinois State Geological Survey

615 East Peabody Drive
Champaign, Illinois 61820

February 26, 2018

Luminescence dating report for Dr. Alan Kehew and John Esch, from the Western Michigan University.

ISGS code	Sample	Equivalent dose (Gy)	Dose rate (Gy/ka)	Age (ka)	n (accepted/total)	Mineral
563	STJ-17-01	36.1 ± 1.4	1.30 ± 0.06	27.9 ± 1.7	59/240	Quartz
564	STJ-17-02	44.3 ± 1.3	1.67 ± 0.07	26.6 ± 1.4	79/240	Quartz

Optically stimulated luminescence (OSL) dating was measured on quartz (150 – 250 μm) or K-feldspar (150 – 180 μm) grains, on very small aliquots. The K-feldspar age was corrected for anomalous fading. Uncertainties are reported at a 1σ significance, providing a level of confidence of approximately 67%. The uncertainties combine random and systematic errors, added in quadrature.

Further details can be found in the report.

Sebastien Huot, Ph.D.
Illinois State Geological Survey
Champaign, Illinois
shuot@illinois.edu
+1-217-300-2579 (office)

This is a report on the optically stimulated luminescence (OSL) dating of four samples sent delivered to us by Alan Kehew and John Esch, in July - August, 2017. The samples were retrieved in opaque tubes from natural exposure. The depositional environment are interpreted as lacustrine (STJ-17-0x) or outwash (DIC-17-01). For the purposes of internal identification, we labeled these samples ISGS 563 to 566.

1. Sample preparation and equipment

The tubes were opened and the mineral extraction was conducted in a subdued orange light environment. Two inch of sediment was removed from both ends of the tube because these might have been partially exposed to light during sampling. Sediment from the external portions was used to measure the *in situ* water content and its radioactive content (uranium, thorium, and potassium), both for dose rate calculation. Quartz and K-feldspar minerals for OSL dating were extracted from the remainder (inner portion) of each tube.

These minerals were wet sieved to retrieve the 150- to 250-µm grain size. A hydrochloric acid attack (HCl, 10%) was applied to dissolve any carbonate minerals that might be present. Using a heavy liquid solution (2.58 g/mL) of lithium heteropolytungstate (LST), we separated K-feldspar (<2.58) from the quartz minerals (>2.58). For quartz, further purification was done with a hydrofluoric acid (HF) attack (48% for 1 hour) to dissolve any remaining impurities. A second HCl attack was performed to dissolve calcium fluorite minerals, a potential by-product of HF dissolution of Ca-rich silicates. Finally, the purified quartz extracts were again sieved, at 150 µm, to remove partially dissolved impurities. A purity check was performed by doing an infrared over blue OSL stimulation. These quartz samples showed no significant contamination from feldspar. For K-feldspar minerals, these were further sieved (dry) at the 150- to 180-µm grain size.

To obtain the dose rate, sediments from the external portion of each sampling tube were dried, and a representative portion was encapsulated in petri dishes (~20 g) and sealed with paraffin wax. A minimum waiting time of 21 days after sealing is recommended to restore the radioactive equilibrium of radon-222 daughter products (Gilmore, 2008). The specific activities (Bq/kg) were measured with a broad-energy high-purity germanium detector (BEGe), in a planar configuration, shielded by 15 cm of lead. Efficiency calibration of the detector was obtained with a set of four certified standards (IAEA-RGU-1, IAEA-RGTh-1, IAEA-RGK-1, and IAEA-385).

2. Equivalent dose (De) measurements

For the equivalent dose (De) measurements, we relied on an automated Lexsyg Smart system equipped with a set of green (525-nm) and infrared (850-nm) LEDs for light stimulation. Detection was done in UV-blue light (combination of Schott BG3 glass and Delta BP 365/50 EX interference filters) for quartz or in blue light (combination of Schott BG39 glass and Semrock 414/46 Brightline HC interference filters) for K-feldspar. For each quartz sample, we dispensed grain over a 6 mm diameter area, centered onto a silicon oil-covered stainless steel cup (10 mm in diameter). Even with so many grains the OSL signal intensity was very dim, frequently yielding no discernable signal from the instrumental background. For K-feldspar, we dispensed one grain on each cup, centered onto a silicon oil covered stainless cup (10 mm diameter).

OSL measurements were carried out with a single-aliquot regenerative dose (SAR) protocol (Table 1). The optimal measurement parameters were selected by a dose recovery test (latent dose bleached with twice with a green LED exposure, at 125°C). An initial dose was given at first (that was a close match to the measured equivalent dose for each sample; 44 or 35 Gy, for quartz or K-feldspar) and it was subsequently recovered by measuring its equivalent dose with the SAR protocol (Figure 1). The samples responded well to the treatment. The optimal measurement treatment was verified for all sample. From this we selected a preheat temperature (Lx) of 240°C (held for 10 seconds) or 200°C (held for 60 seconds), for quartz or K-feldspar. The preheat temperature for the test dose (Tx) was 200°C or 200°C (held for 60 seconds), for quartz or K-feldspar. The dose recovery test gave an average measured-to-given dose ratios of 0.962 ± 0.013 or 1.019 ± 0.014, for quartz or K-feldspar. This outcome is positive. Considering this result, we opted to select the parameters in Table 1.

Table 1a. Measurement steps for the single-aliquot regenerative protocol (Murray and Wintle, 2000; 2003)[1]

Step	Procedure (quartz)
1	Regeneration[1]/natural dose
2	Preheat (240°C), hold for 10 seconds
3	OSL stimulation with green LEDs at 100°C for 35 seconds (L_x)
4	Test dose beta irradiation (22 Gy)
5	Preheat (200°C) for 0 seconds
6	OSL stimulation with green LEDs at 100°C for 35 seconds (T_x)
7	Repeat Steps 1–6 with further regeneration doses

[1] For equivalent dose measurements, we gave a range of laboratory-induced doses that would properly encompass the variability of the observed natural luminescence.

Table 1b. Measurement steps for the single-aliquot regenerative protocol (Huot and Lamothe, 2003; Murray and Wintle, 2000; 2003)[1]

Step	Procedure (feldspar)
1	Regeneration[1]/natural dose
2	Preheat (200°C), hold for 60 seconds
3	Pause[2]
4	IRSL stimulation with IR LEDs at 50°C for 100 seconds (L_x)
5	Green and IR LEDs bleaching for 30 seconds
6	Test dose beta irradiation (4 Gy)
7	Preheat (200°C) for 60 seconds
8	IRSL stimulation with IR LEDs at 50°C for 100 seconds (T_x)
9	Green and IR LEDs bleaching for 30 seconds
10	Repeat Steps 1–9 with further regeneration doses

[1] For equivalent dose measurements, we gave a range of laboratory-induced doses that would properly encompass the variability of the observed natural luminescence.

[2] There was no pause for equivalent dose measurements. A pause was observed here for anomalous fading measurements.

For the equivalent dose, all calculations were made using the "late light" approach for background subtractions, by taking the initial 20 data channels (10 seconds) from the OSL decay curve and removing the background from the end of the stimulation curve (25 data channels, 12.5 seconds; Figure 2). Quartz aliquots were rejected (Table 2) because of feldspar contamination (10% threshold limit), high recuperation (5% limit of the natural luminescence) or recycling ratio (10% threshold limit). In addition,

few aliquots were rejected for having a low fast-ratio (OSL decay shape; Durcan and Duller, 2011). The laboratory-induced luminescence growth curve was not able to reach the level of the natural luminescence ratio (Ln/Tn) before reaching saturation, for some aliquot. This is a documented phenomenon in single grain dating of quartz which remains unexplained (De > sat; Wintle and Murray, 2006). Most aliquots were rejected as their either had no discernable OSL intensity from the instrumental background (no signal) or had a very low intensity (signal too close to background).

For K-feldspar, all calculations were made using the "late light" approach for background subtractions, by taking the initial 5 data channels (5 seconds) from the IRSL decay curve and removing the background from the end of the stimulation curve (30 data channels, 30 seconds; Figure 2d). Some aliquots were rejected due to the failure in the recycling ratio (10% threshold limit), while others aliquots had no discernable IRSL intensity or a very low intensity above the background.

2.1 Equivalent dose calculation

Uncertainties relied on Poisson statistics. For curve fitting, we also propagated the uncertainties from the optimized luminescence growth curve parameters. In addition, when the observed scatter about the best fit regression line was too high, the uncertainties were increased (Figure 3). For this, we relied on the one-tailed probability χ^2 distribution, with $N - 3$ degrees of freedom (where N is the number of measured data points). When the probability was lower than 15% (i.e., the data points scattered above and beyond the best fit line), the uncertainties for the optimized parameters were expanded by Student's *t* values for $N - 3$ degrees of freedom (Brooks et al., 1972; Ludwig, 2003).

2.2 Anomalous fading

Anomalous fading measurements were performed on the same aliquot previously used for equivalent dose measurements. After the equivalent dose measurement cycles, the aliquots were taken outside the luminescence system, for sunlight bleaching (2 days), before passing over the anomalous fading sequence of measurements. It also employed the SAR protocol (table 1), with two adjustments. The laboratory-induced dose (step 1) was fixed, at 52 Gy, along with a test dose (step 6) of 22 Gy. Also, there was a 'pause' in effect, at step 3, which ranged from 0.1 up to 70 hours (Figure 4). Fading corrected ages relied on the model proposed by Huntley and Lamothe (2001).

Table 2. Tally of rejected aliquots.

ISGS code	Sample	n (accepted/total)	feldspar contaminated	recuperation	recycling	OSL decay shape	De > sat	signal too close to background	no signal
563	STJ-17-01	59/240	9	3	3	–	8	46	112
564	STJ-17-02	79/240	4	1	2	1	11	49	93

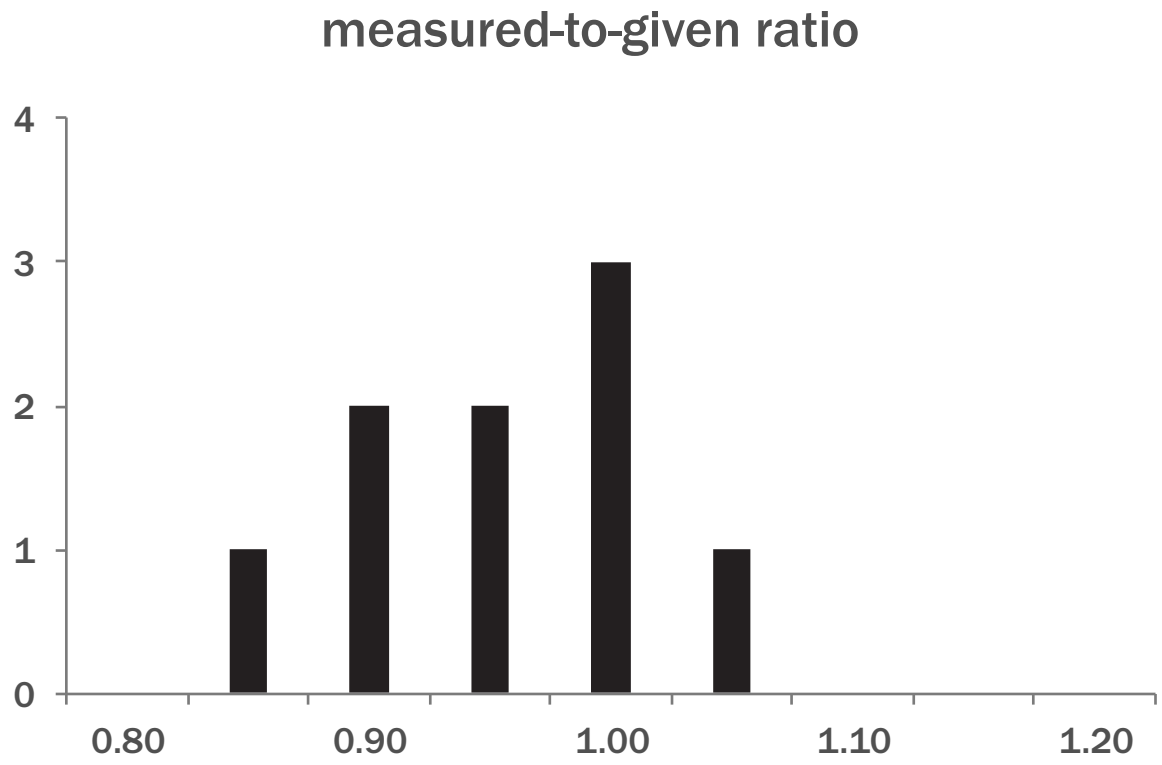

Figure 1. Summary for the dose recovery for every sample, for its selected and retained preheat temperature (Table 1). The weighted average ratio is 0.962 +/- 0.013 and 1.019 +/- 0.014, for quartz and K-feldspar. Luminescence dating tolerance tends to be conservative. For the dose recovery, we allow up to 10% variation from unity (i.e., 0.9 – 1.1).

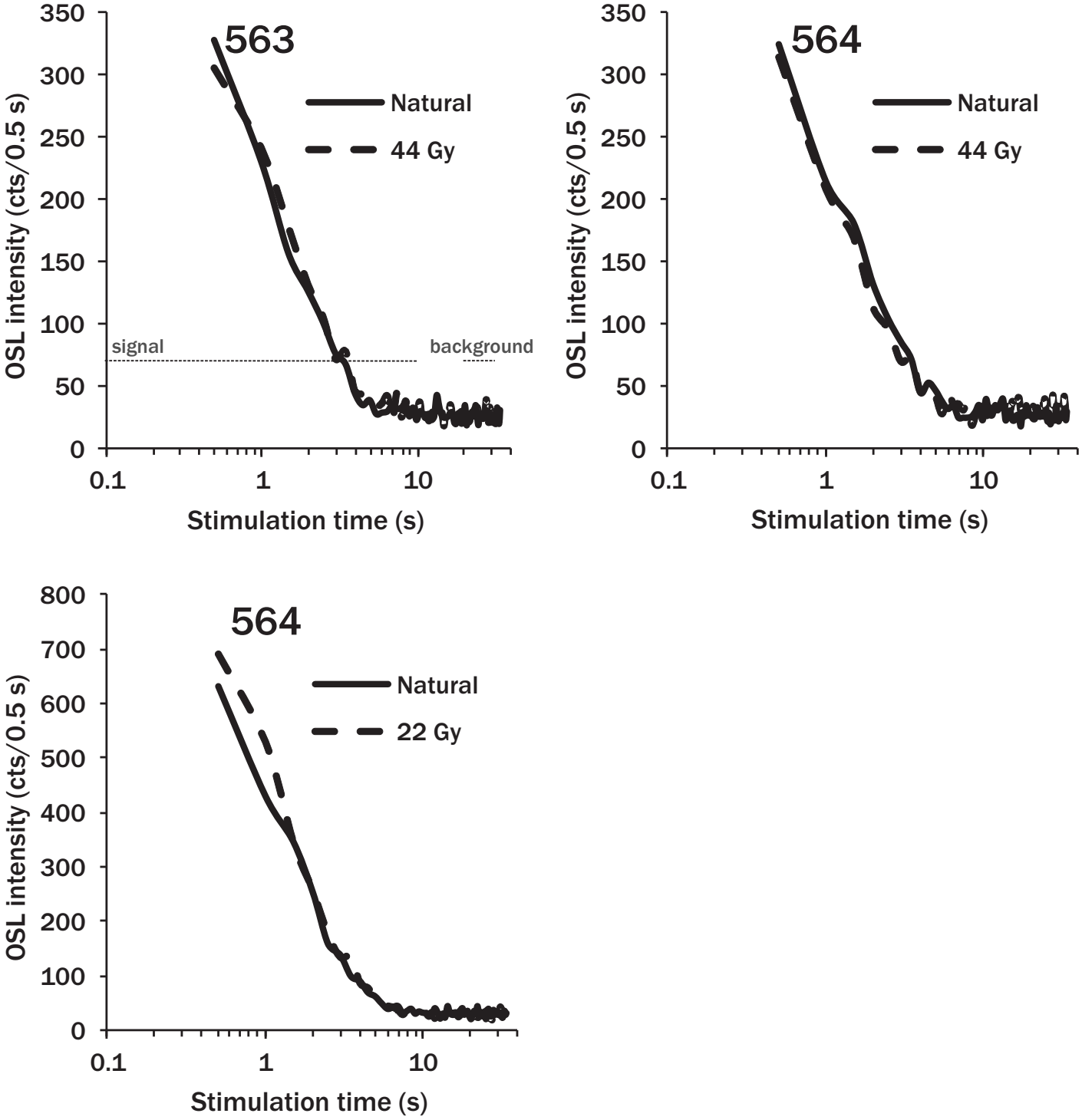

Figure 2. Typically OSL decay curve, for a naturally dose aliquot (solid curve) or laboratory-induced dose (dashed curve, in Gy). The area under the curve is proportional to the dose of radiation stored within the mineral. Their luminescence growth curve are shown in Figure 3.

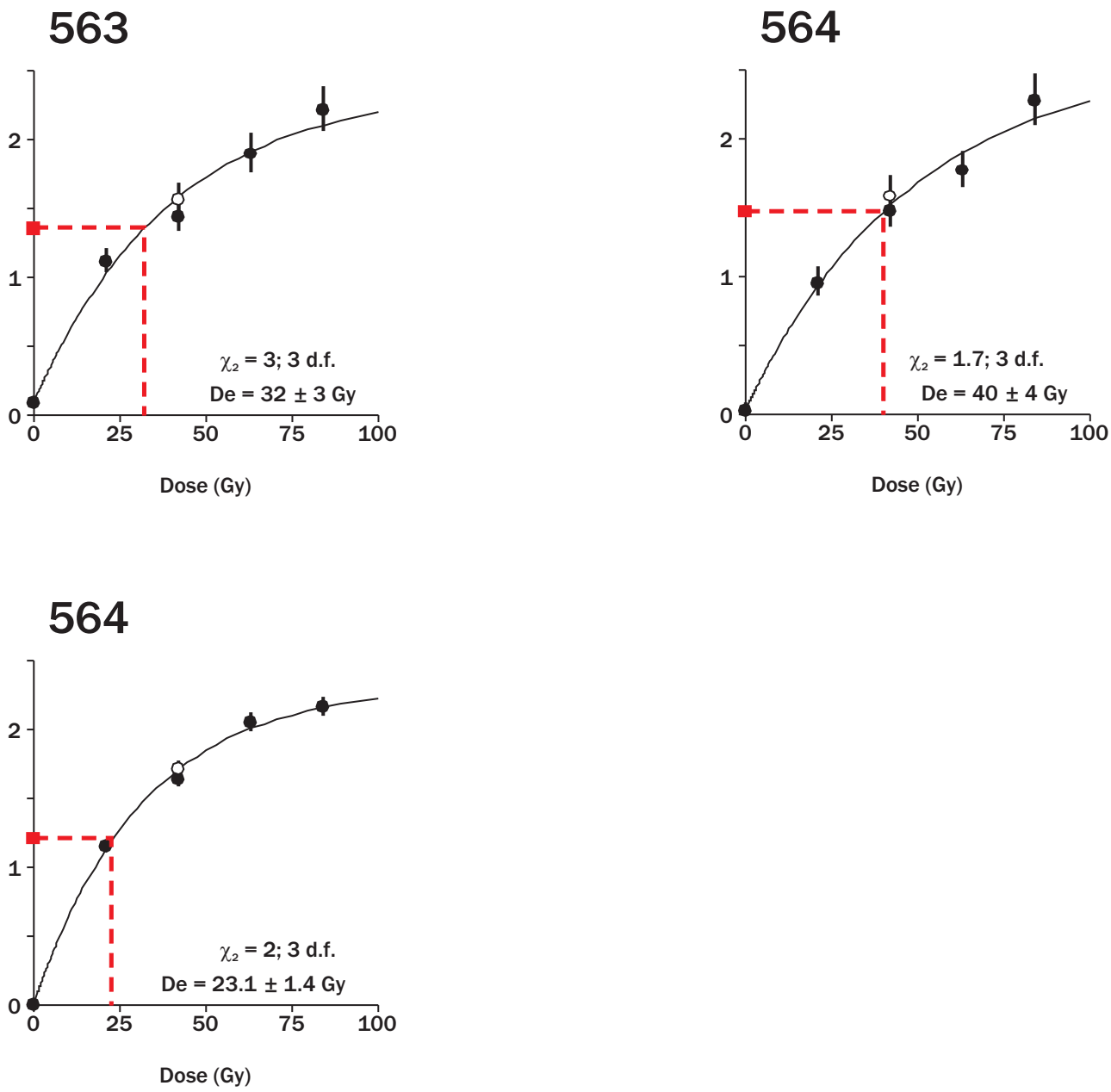

Figure 3. Luminescence dose response curve for the same aliquots shown in Figure 2. Each point corresponds to the OSL (Lx; measurement step 3) of a natural (red square) or laboratory-induced dose (filled circles)), normalized by the luminescence response to a fixed test dose (Tx; measurement step 6). A repeat measurement (the recycling test; open circles) was performed at the end. The equivalent dose is obtained by interpolation. For the aliquots shown here, the observed measurements scatter well around the predicted best-fit curve.

2.3 Age distribution

A weighted average (using the central age model; Galbraith et al., 1999) was used in all calculations. The central age model provides an overdispersion parameter. This parameter characterizes the degree to which the observed weighted distribution is consistent with the predicted weighted distribution from the observed data. At 0%, the observed distribution is equal to the statistical prediction. In luminescence dating, it is common for the observed distribution to be slightly larger than the expected distribution by a value of approximately 20%. This means that the calculated uncertainties tend to underestimate the "real" uncertainties because of intrinsic (e.g., instrumental uncertainties, luminescence characteristics of quartz and K-feldspar) or extrinsic (e.g., partial bleaching, external beta microdosimetry) factors. The central age model expands the age uncertainty in an attempt to account for this discrepancy. Here, the overdispersions are above average for all samples (Table 3), especially for STJ-17-03. It indicates a large scatter in the calculated age distribution (Figure 5).

Table 3. Age overdispersion parameters[1]

ISGS code	Sample	Overdispersion (%)
563	STJ-17-01	29 ± 4
564	STJ-17-02	29 ± 4

[1]A value of 20% is typical in luminescence.

Sample STJ-17-03 displays a significant broadness in its age distribution (Figure 5). The age distributions for samples STJ-17-01 and -02 are not as broad, but it is still significant. DIC-17-01 is reasonably well-distributed, despite the scatter. To document the shape of the age distribution more clearly, we must reduce the number of quartz (or K-feldspar) grains dispensed on each aliquot. Otherwise, in the presence of a multitude of grains on one aliquot (some being well bleached and others not; alternatively, from two distinct events, of different ages), each emitting a luminescence light signal, all these would add up to give an average, overestimated age compared to the most recent geological event that brought these quartz grains inside the sand wedge (Arnold and Roberts, 2009). The only recourse here is to reduce the number of grains dispensed on the aliquot (Olley et al., 1999). At the extreme limit, we would measure the luminescence from a single grain.

Usually, the best age estimate should rely on the average value from a repeated set of observations. We can think of instances when this might be inappropriate. A positive skewness, such as is noted here for most samples (Figure 5), is a clear sign of partial bleaching. In other words, during the last sedimentary cycle (erosion, transport, deposition, and burial), not all sedimentary grains of sand were sufficiently exposed to sunlight to completely reset the "dosimetric clock" that they had accumulated in their previous burial setting. Alternatively, it could reflect a population mixture of different events, formed at different ages, but with the most predominant population coming from the more recent event.

Although the mean is the scientist's best friend, it might prove to be an inappropriate estimator in this situation. Here, we opted to rely on the minimum age model (Galbraith et al., 1999). We chose to add an additional uncertainty (σb; 10%), in quadrature, to each individual aliquot before inserting the aliquots

into the minimum age model to account for intrinsic and extrinsic uncertainties which cannot be properly quantified (Figure 6; Table 4).

Table 4. Burial age comparison between the weighted mean (central age model) and minimum age model (MAM).

ISGS code	Sample	Weighted mean (ka)	MAM (ka)
563	STJ-17-01	34 ± 2	27.9 ± 1.7
564	STJ-17-02	27.9 ± 1.7	26.6 ± 1.4

As a clarification, the model is thus named: minimum age model. It is not a lower "boundary age". It should be considered instead as the best age estimate, reflective of the geological burial age for the last sedimentary event.

For K-feldspar (DIC-17-01, 566), only 13 (of the 25 aliquot) had a paired equivalent dose and fading rate measured. For the remaining 12 aliquots, we only measured the equivalent dose and relied on an average fading rate (0.21 +/- 0.14 %/decade) for the fading correction (dashed circles; Figure 5).

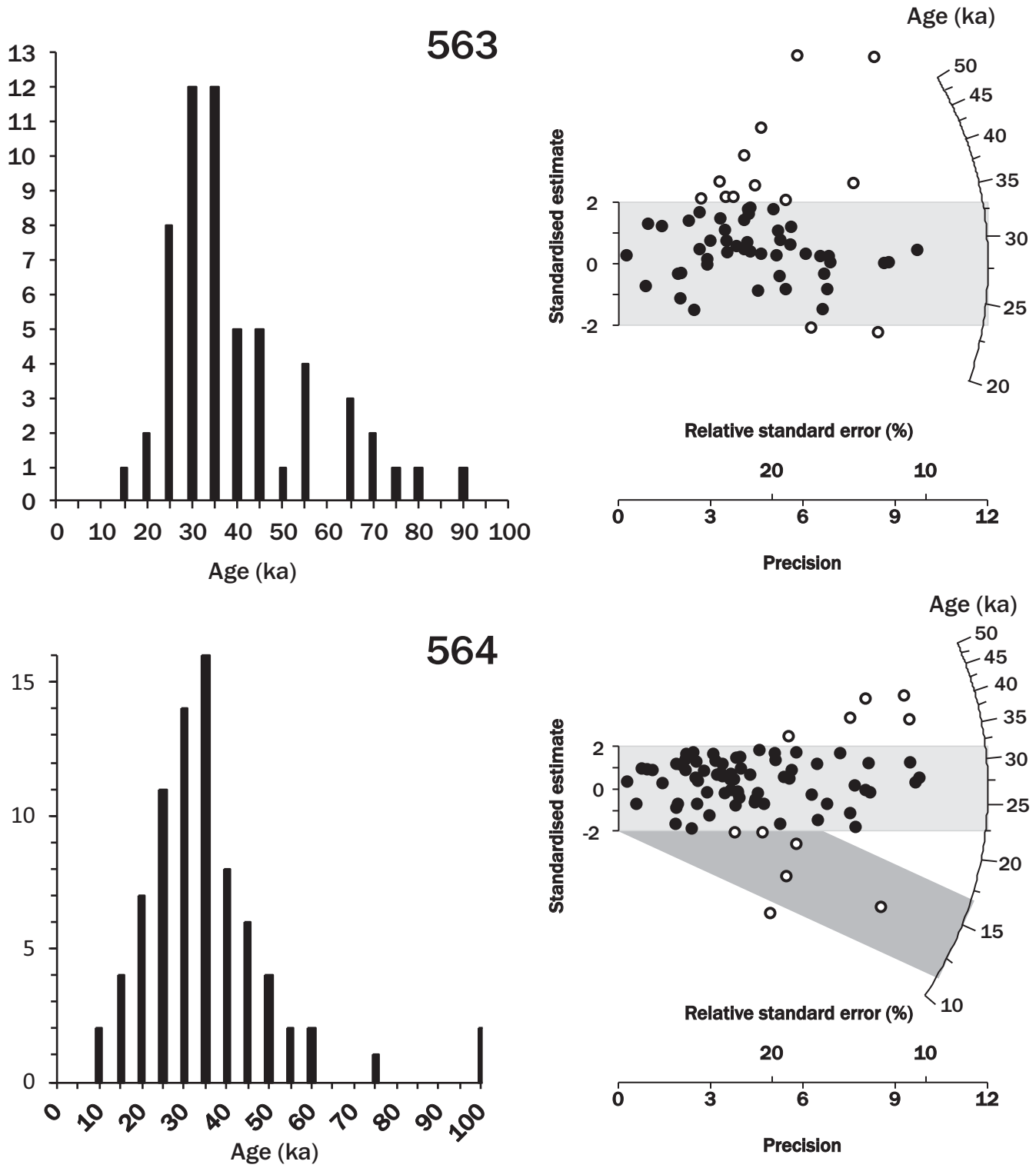

Figure 5. Age distributions, as an histogram and a radial plot, for all samples. Each circle on the radial plot represents the age and uncertainty, for a single aliquot. The age is read on the arc axis, by drawing a straight line from (0,0), passing through a circle and intersecting the radial axis (log scale). The (0,0) coordinate corresponds to a 0 standardised estimate (y-axis) and 0 precision (x-axis). The uncertainty is read on the horizontal axis, by drawing a perpendicular line reaching a circle. Hence, two aliquots, having the same age, but with different uncertainty, will lay on the same straight line (from (0,0) to the radial axis). The aliquot with the smaller uncertainty (higher precision) will be closer to the arc. Values (filled circles) within the light grey shaded band are consistent (at 2σ) with the weighted mean (Central Age Model). A cluster of aliquots within this shaded band expresses confidence that we have a population of grains consistent with a single age.

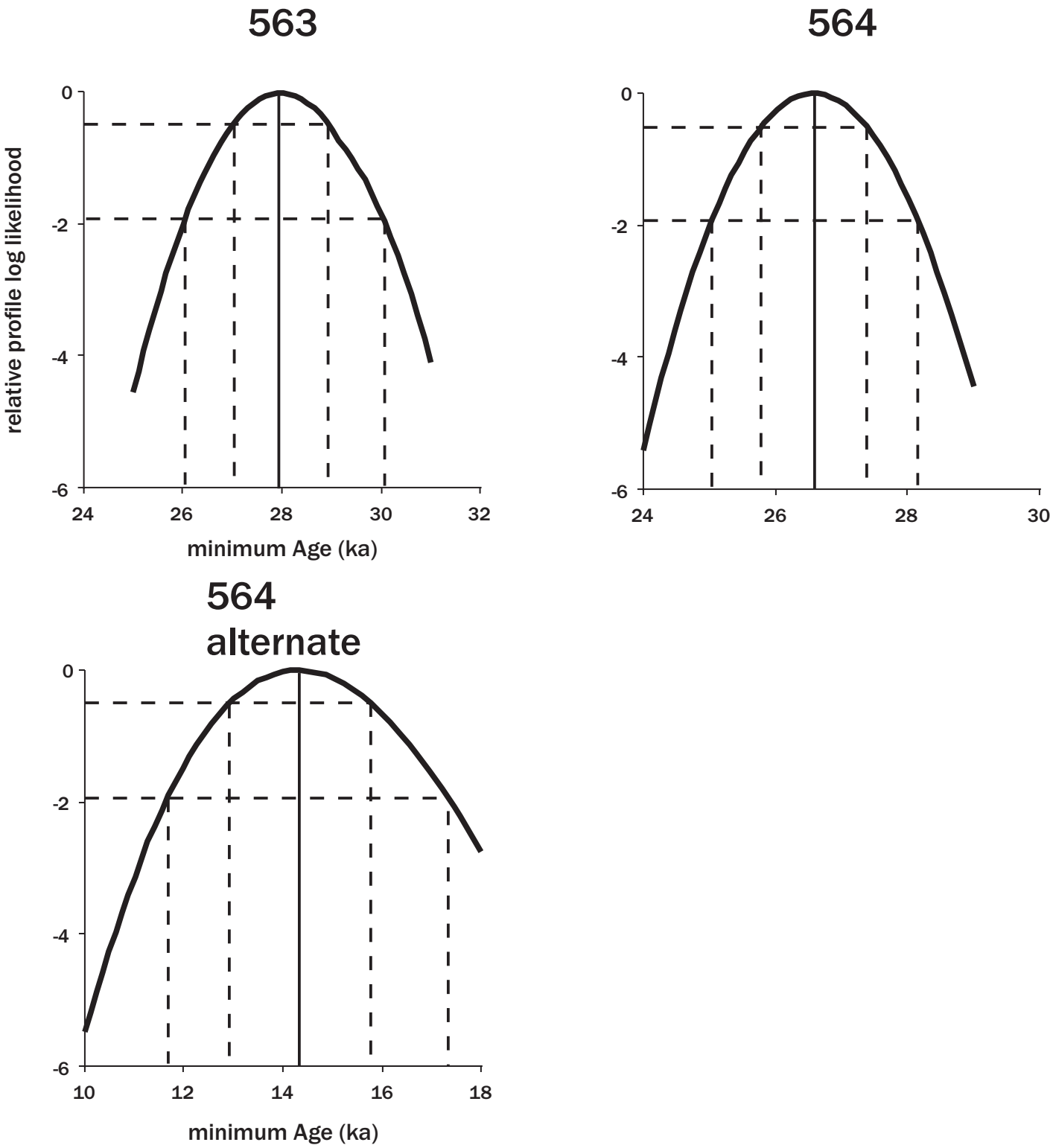

Figure 6. Relative profile log likelihood. The minimum age is found at the maximum value of the profile (solid vertical line). The 1σ and 2σ age uncertainties are shown by the dashed lines intersecting the profile, at a 0.5 and 1.92 relative likelihood.

3. Dose rate

The water content was measured for each sample. The as-received water content was very dry, except for STJ-17-02 (Table 5). We retained a value of 5 % for the age calculation, for STJ-17-03 and DIC-17-01. Both STJ-17-01 and -03 were sampled deeper. It would make sense that these two would have a higher water content throughout their burial history. The water content for STJ-17-01 was increased to 10 %, to take into account the field notes ("water content higher than STJ-17-01"). We assigned a water content uncertainty of 5 % to account for possible variation during the entire length of burial. The bulk density was measured. It ranged from 1.60 to 1.67 g/cm^3.

Table 5. Water content, measured from the sample, along with the value presumed to have prevailed during the burial

ISGS code	Sample	in situ (%)	presumed (%)
563	STJ-17-01	3	10 ± 5
564	STJ-17-02	14	15 ± 5

Waiting times of 30 to 40 days were observed before measuring the radioactive activities of uranium, thorium, and potassium, from which we can derive contributions from alpha, beta, and gamma energy decay (Table 6, Figure 7).

Table 6. Specific activity (Bq/kg)

ISGS code	Sample	238U	226Ra	210Pb	232Th	40K
563	STJ-17-01	6.6 ± 0.8	7.0 ± 0.2	6.7 ± 1.0	5.90 ± 0.16	357 ± 6
564	STJ-17-02	13.5 ± 1.1	13.1 ± 0.3	10.8 ± 1.3	12.7 ± 0.2	445 ± 7

For quartz, we assumed an internal content of 0.08 ± 0.02 ppm and 0.18 ± 0.03 ppm, for uranium and thorium, respectively (Vandenberghe et al., 2008). A conservative 0.04 ± 0.02 "a value" (efficiency of alpha particles compared with beta particles upon inducing a trapped charge in quartz and feldspar; i.e., alpha is only 4% as effective as beta) was retained. The external alpha dose rate contribution was assumed to be negligible here because we etched the quartz grains (Table 7).

For K-feldspar, we assumed an internal content of 12.5 ± 0.5 % and 400 ± 100 ppm, for potassium and rubidium, respectively (Huntley and Baril, 1997; Huntley and Hancock, 2001). A conservative 0.10 ± 0.05 "a value" (efficiency of alpha particles compared with beta particles upon inducing a trapped charge in quartz and feldspar; i.e., alpha is only 10% as effective as beta) was retained.

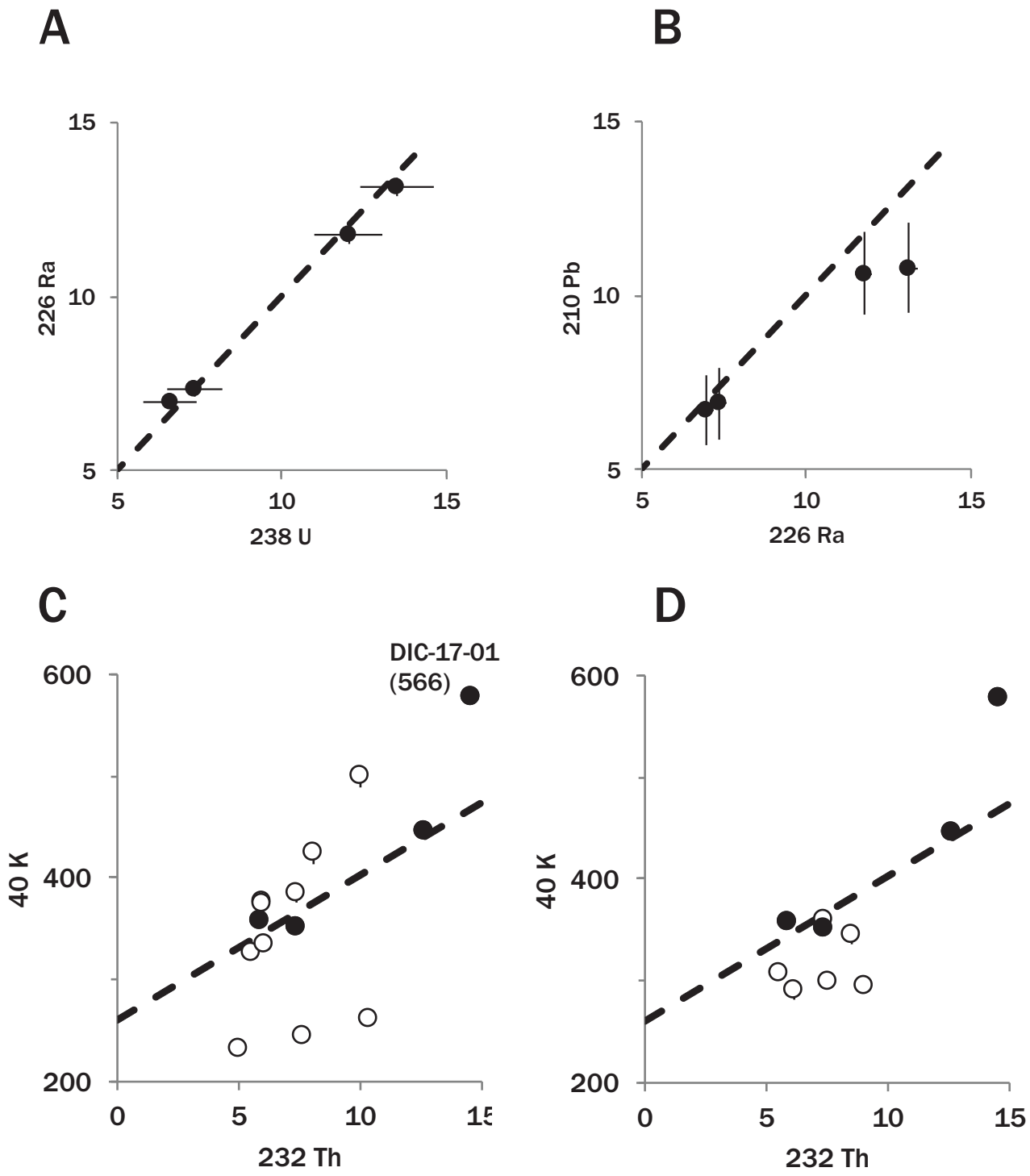

Figure 7. Specific activity (Bg/kg) for uranium 238, radium 226 and lead 210, for all samples. A), relationship of radium 226 versus uranium 238. B), relationship of lead 210 versus radium 226. The dashed line represents the 1:1 ratio (A, B). If a sample is in equilibrium, then the daughter isotope (y-axis) will match the activity of its parent (x-axis). C), relationship of potassium 40 versus thorium 232. The dashed line represents the best-fit for samples 563, 564, 565. The open circles represent previous samples (OSL-CA-15-x, PIRO-15-03, CASS-OSL-16-x). D) Comparison with other outwash sediments (open circles). Uncertainties are shown for 1σ.

Table 7. Contribution to the dose rate, expressed in Gy/ka[1]

ISGS code	beta external	gamma	cosmic ray	depth (m)	bulk density (g/cm3)	water (%)	total
563	0.83 ± 0.06	0.37 ± 0.01	0.08 ± 0.01	9.51	1.61	10 ± 5	1.30 ± 0.06
564	1.04 ± 0.07	0.53 ± 0.02	0.09 ± 0.01	9.19	1.60	15 ± 5	1.67 ± 0.07
565	0.88 ± 0.06	0.41 ± 0.02	0.16 ± 0.01	2.79	1.67	5 ± 5	1.46 ± 0.07

[1] We relied on an internal alpha dose rate of 0.01 ± 0.01 for quartz. For K-feldspar, we relied on an internal alpha and beta dose rate contributions of 0.05 ± 0.01 and 0.67 ± 0.03 Gy/ka, respectively.

The beta dose rate absorption efficiencies were adjusted according to the specific grain size and mineral used for equivalent dose measurement (Nathan, 2011). External beta and gamma contributions were attenuated for water content (Zimmerman, 1971). The energy-to-dose rate conversion coefficient relied on the update by Guérin et al. (2011).

4. Uncertainty budget

The breakdown of the uncertainties, between the total random and systematic sources, are presented in table 8. The random uncertainties reflects the standard error on the best estimate (i.e. from the weighted mean age or the minimum age model) for the equivalent dose (in seconds of laboratory-induced irradiation). The systematic uncertainties reflects here the combine (in quadrature) components of the environmental dose rate and calibration of the beta source on the luminescence system.

Table 8. Random and systematic uncertainties (in ka), at 1 sigma.

ISGS code	Sample	Age (ka)	1σ (random)	1σ (systematic)
563	STJ-17-01	27.85 ± 1.73	± 1.08	± 1.36
564	STJ-17-02	26.57 ± 1.44	± 0.80	± 1.20

5. Interpretation

Sample STJ-17-02

There is a weak possibility that the burial age for this sample to be younger, at 14.3 ± 0.6 ka. There is one, exceptional, quartz grain (Figure 2 and 3, natural ~ 23 Gy) that behaved well and emitted a decent amount of luminescence signal. On the age distribution (Figure 5), the darker shaded rectangle (radial plot) encompass that younger age.

My interpretation of the age distribution still rest on the 26.6 ± 1.4 ka (minimum age model). The age distribution is well-defined around that age. It is also, this younger mode, 14.3 ka, rests entirely on 1 aliquot. There are two or three additional aliquots (in the darker shaded rectangle), but these have higher uncertainties.

The minimum age for STJ-17-02 is a very close match to STJ-17-01 (27.9 ± 1.7 ka). If we calculate the P-value between these two ages (using the random uncertainties, Table 8), we get a value of 33 %. There are thus undisguisable.

I understand that these ages are older than what you had anticipated. I completed my analysis before I refreshed my mind with the glacial geology interpretation that had been provided with the samples (the less I know, the more objective I am!). Without giving too much detail, you may remember Bill Monaghan's presentation during the last Coalition meeting (Pennsylvania, 2017). He was a bunch of outwashes sediments, some in the North West corner of Indiana. The ages were older than what he anticipated. Steve Brown commented that, for him, they were supporting a different pattern of deglaciation and what quite please by these ages. The ages for STJ falls in the same age range. Also of interest, these various samples more or less cluster together in the potassium vs thorium scatter (Figure 7d). This suggest a common (mixture) of source(s) sediment.

6. Conclusion

In summary, the samples were well-behaved in their luminescence light-response, but had a low luminescence intensity.

Sebastien Huot
Visiting Research Scholar - Geochemistry
Illinois State Geological Survey

References

Brooks, C., Hart, S.R., Wendt, I., 1972. Realistic use of two-error regression treatments as applied to rubidium-strontium data. Reviews of Geophysics 10, 551-577.

Durcan, J.A., Duller, G.A.T., 2011. The fast ratio: A rapid measure for testing the dominance of the fast component in the initial OSL signal from quartz. Radiation Measurements 46, 1065-1072.

Galbraith, R.F., Roberts, R.G., Laslett, G.M., Yoshida, H., Olley, J.M., 1999. Optical dating of single and multiple grains of quartz from Jinmium rock shelter, northern Australia: part I, experimental design and statistical models. Archaeometry 41, 339-364.

Gilmore, G.R., 2008. Practical gamma-ray spectrometry, 2nd ed. John Wiley & Sons, Ltd.

Guérin, G., Mercier, N., Adamiec, G., 2011. Dose-rate conversion factors: update. Ancient TL 29, 5-8.

Huntley, D.J., Baril, M.R., 1997. The K content of the K-feldspars being measured in optical dating or in thermoluminescence dating. Ancient TL 15, 11-13.

Huntley, D.J., Hancock, R.G.V., 2001. The Rb contents of the K-feldspar grains being measured in optical dating. Ancient TL 19, 43-46.

Huntley, D.J., Lamothe, M., 2001. Ubiquity of anomalous fading in K-feldspars and the measurement and correction for it in optical dating. Canadian Journal of Earth Sciences 38, 1093-1106.

Huot, S., Lamothe, M., 2003. Variability of infrared stimulated luminescence properties from fractured feldspar grains. Radiation Measurements 37, 499-503.

Ludwig, K.R., 2003. Mathematical-statistical treatment of data nd errors for Th-230/U geochronology, In: Bourdon, B., Henderson, G.M., Lundstrom, C.C., Turner, S.P. (Eds.), Uranium-Series Geochemistry. Mineralogical Society of America, pp. 631-656.

Murray, A.S., Wintle, A.G., 2000. Luminescence dating of quartz using an improved single-aliquot regenerative-dose protocol. Radiation Measurements 32, 57-73.

Murray, A.S., Wintle, A.G., 2003. The single aliquot regenerative dose protocol: potential for improvements in reliability. Radiation Measurements 37, 377-381.

Nathan, R.P., 2011. Numerical modelling of environmental dose rate and its application to trapped-charge dating. University of Oxford, Oxford, UK, p. 207.

Vandenberghe, D., De Corte, F., Buylaert, J.P., Kučera, J., Van den haute, P., 2008. On the internal radioactivity in quartz. Radiation Measurements 43, 771-775.

Wintle, A.G., Murray, A.S., 2006. A review of quartz optically stimulated luminescence characteristics and their relevance in single-aliquot regeneration dating protocols. Radiation Measurements 41, 369-391.

Zimmerman, J., 1971. The radiation-induced increase of the 100°C thermoluminescence sensitivity of fired quartz. Journal of Physics C: Solid State Physics 4, 3265-3276.